



**Universidade do Minho**  
Escola de Engenharia

Diana Raquel Carvalho da Costa

**Study of blood cells flowing in microchannels with  
diverging bifurcations and development of an  
innovative blood analogue fluid**

Master Thesis

Integrated Master in Biomedical Engineering

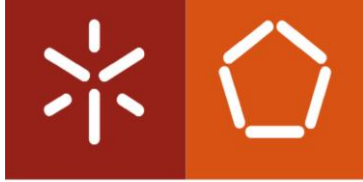
Dissertation made with supervision of:

Professor Rui Alberto M.M. Lima

Professor Stefan Gassmann

December of 2018





**Universidade do Minho**  
Escola de Engenharia

Diana Raquel Carvalho da Costa

**Study of blood cells flowing in microchannels with  
diverging bifurcations and development of an  
innovative blood analogue fluid**

Master Thesis

Integrated Master in Biomedical Engineering

Dissertation made with supervision of:

Professor Rui Alberto M.M. Lima

Professor Stefan Gassmann

Professor Pablo Fuciños

Professor Isabel Amado



December of 2018



## DECLARAÇÃO

Nome: Diana Raquel Carvalho da Costa

Endereço eletrónico: dianarccosta@gmail.com Telefone: 912435312

Bilhete de Identidade/Cartão do Cidadão: 14586231

Título da dissertação: Study of blood cells flowing in microchannels with diverging bifurcations and development of an innovative blood analogue fluid.

Orientadores:

Professor Doutor Rui Alberto M.M. Lima

Professor Doutor Stefan Gassmann

Ano de conclusão: 2018

Mestrado Integrado em Engenharia Biomédica

É AUTORIZADA A REPRODUÇÃO INTEGRAL DESTA DISSERTAÇÃO APENAS PARA EFEITOS DE INVESTIGAÇÃO, MEDIANTE DECLARAÇÃO ESCRITA DO INTERESSADO, QUE A TAL SE COMPROMETE.

Universidade do Minho, \_\_\_\_/\_\_\_\_/\_\_\_\_\_

Assinatura:



## ACKNOWLEDGMENTS

Without the contribution of some people this work would not be possible and for that I would like to express my gratitude.

First of all, I would like to thank my advisers, Professor Rui Lima and Professor Stefan Gassmann, and to the laboratory technician Helmut Schüttle for all the support, knowledge they shared with me to improve my work and also for providing me an incredible experience in Germany.

I would like to thank Pablo Fuciños and Isabel Amado for their orientation, availability and friendliness during my work at INL to develop the blood analogue fluid.

To Engineer Raquel Lopes my gratitude for the support during this work and for making me feel at home during my stay in Germany.

To the people who shared the Erasmus experience with me, thank you. Thanks also to all the people at Jade University of Applied Sciences, they were very helpful and friendly.

I thank my friends for the incredible years of academic life. The past few years have been incredible. Special thanks to my partners Vera Gonçalves and Beatriz Leão for the last few years, but especially for their support during this work.

Finally, I would like to thank my family. The most special thanks to my parents, Abílio and Glória, for always believing, encouraging and being my best friends, and to my brother, Nuno, for always worrying. Everything I've become is owed to them.

Additionally, I would like to acknowledge the support of the following projects:

POCI-01-0145-FEDER-016861 (PTDC/QEQ-FTT/4287/2014), NORTE-01-0145-FEDER-029394 (PTDC/EMD-EMD/29394/2017), NORTE-01-0145-FEDER-030171 (PTDC/EMESIS/30171/2017) and NORTE-01-0145-FEDER-028178 (PTDC/EEI-EEE/28178/2017), funded by COMPETE2020, NORTE2020, PORTUGAL2020 and FEDER.





## ABSTRACT

Blood is a non-Newtonian fluid made up of different types of cells, platelets and a yellowish liquid called plasma and it is essential for the diagnosis of various diseases. Blood flow is a topic of great interest to the scientific community and therefore several studies have been done using microfluidic devices to mimic the microvascular system. As the experiments with real blood are often complex due to safety, economical and bureaucratic issues, the research about the development of blood-like fluids has been during the years an important research topic.

In the first phase of this work, a blood analog was developed using the Encapsulator B-395 Pro and alginate to produce flexible microparticles to mimic the red blood cells (RBCs). To reach the goal, different procedures were tested. Overall, the results were satisfactory.

In a second phase, microchannels in polydimethylsiloxane (PDMS) were manufactured using a soft lithography technique. The master molds in SU-8 were manufactured by photolithography and well-defined complex structures were obtained. These microchannel networks aimed to study the flow behavior of individual RBCs at diverging bifurcations.

Finally, individual RBCs were studied in microchannels having diverging bifurcations with different angles. The deformation and velocity of RBCs were measured by using a high-speed video microscopy system. Overall, the results clearly indicate that the stagnation region located at the bifurcation apex strongly influence both RBCs velocity and deformability. Additionally, around the apex the cells in addition to the increase of the deformation also seem to suffer a rotational motion.

This work provides an important contribution to the field of blood analogues, microfluidics and microcirculation.

**KEYWORDS:** Red Blood Cells, Microfluidics, Microcirculation, Blood Analogues, Biofluids, Microchannels, Bifurcations, Photolithography, Soft Lithography.



## RESUMO

O sangue é um fluido não newtoniano constituído por diferentes tipos de células, plaquetas e um líquido amarelado chamado plasma e é essencial para o diagnóstico de várias doenças. O escoamento sanguíneo é um tema de grande interesse para a comunidade científica e por isso vários estudos têm sido feitos recorrendo a dispositivos microfluidicos para imitar o sistema microvascular. Como os experimentos com sangue são frequentemente complexos devido a questões de segurança, económicas e burocráticas, a investigação sobre o desenvolvimento de fluidos análogos ao sangue tem sido, durante anos, alvo de investigação.

Numa primeira fase deste trabalho, foi desenvolvido um análogo ao sangue recorrendo ao equipamento Encapsulator B-395 Pro e ao Alginato para fabricar micropartículas a imitar os glóbulos vermelhos. Para se atingir o objetivo testaram-se diferentes procedimentos. De uma forma geral os resultados foram satisfatórios.

Numa segunda fase foram fabricados microcanais em polidimetilsiloxano (PDMS) recorrendo à técnica litografia suave. Os moldes master em SU-8 foram fabricados por fotolitografia e obtiveram-se estruturas bem definidas. Estes microcanais tinham como objetivo o estudo do comportamento do escoamento de glóbulos vermelhos individuais em bifurcações divergentes.

Por último, os glóbulos vermelhos foram estudados individualmente em microcanais que continham bifurcações divergentes com diferentes ângulos. Mediu-se a deformação e velocidade dos glóbulos vermelhos recorrendo a uma câmara de alta velocidade e a um microscópio. No geral, os resultados indicam claramente que a região de estagnação localizada no ápex da bifurcação influencia fortemente a velocidade e deformação dos glóbulos vermelhos. Além disso, em torno do ápex, as células, além do aumento da deformação, também parecem sofrer um movimento de rotação.

Este trabalho fornece uma importante contribuição para a área dos fluidos análogos ao sangue, microfluidica e microcirculação.

Palavras-Chave: Glóbulos Vermelhos, Microfluidica, Microcirculação, Análogo ao Sangue, Biofluidos, Microcanais, Bifurcações, Fotolitografia, Litografia Suave.



## CONTENTS

Acknowledgments.....	vii
Abstract.....	ix
Resumo.....	xi
List of Figures.....	xv
List of Tables.....	xvii
Nomenclature.....	xix
1. Introduction .....	1
1.1 Objectives and Motivation .....	1
1.2 Structure.....	2
2. Theoretical Fundamentals .....	3
2.1 Cardiovascular system .....	3
2.2 Blood properties and flow phenomena .....	4
2.2.1 Hematocrit .....	4
2.2.2 Blood Rheology and Hemodynamics .....	5
2.2.3 Blood Flow behavior in Microchannels.....	7
2.3 Blood analogue fluids .....	10
2.4 Microfabrication of biomedical microdevices .....	11
2.4.1 Photolithography.....	12
2.4.2 Soft lithography .....	14
3. Development of a blood analogue fluid .....	16
3.1 Materials and Methods .....	16
3.2 Presentation and discussion of results .....	19
3.2.1 Test 1.....	19
3.2.2 Test 2.....	22
3.2.3 Test 3.....	23
3.3 Conclusions .....	24
4. Fabrication of microchannels with diverging bifurcations .....	25

4.1	Materials and Methods .....	26
4.1.1	Photolithography.....	26
4.1.2	Soft lithography .....	30
4.2	Results and Discussion.....	31
4.2.1	Photolithography.....	31
4.2.2	Soft lithography .....	34
4.3	Conclusions .....	35
5.	Study of blood flow in microchannels with diverging bifurcations .....	36
5.1	Materials and Methods .....	36
5.2	Results and Discussion.....	37
5.3	Conclusions .....	44
6.	Conclusions and Future work .....	45
6.1	Conclusions .....	45
6.2	Future work.....	46
	Bibliografia .....	47
	Annex I – SU-8 Datasheet.....	51
	Annex II – All Geometries of microchannels produced at Jade University of Applied Sciences .....	56

## LIST OF FIGURES

Figure 1: Composition of blood [5].	3
Figure 2: Hematocrit for different conditions [7].	5
Figure 3: Newtonian and non-Newtonian fluids [10].	6
Figure 4: Relation between viscosity and shear rate of water (0% Hct), normal RBCs (45% Hct) suspended in plasma and hardened RBC's [11].	6
Figure 5: Schematic diagram showing the changes in blood pressure and Re on the large arteries, capillaries and veins [12].	8
Figure 6: Separation of the cells in the bifurcations [14].	9
Figure 7: Scheme showing the influence of the hematocrit on the separation phase of RBCs. [13].	9
Figure 8: Flow of Red Blood Cells (left side) and blood analogue fluid with PMMA particles (right side) through a hyperbolic microchannel [19].	11
Figure 9: Scheme of spinning [25].	13
Figure 10: Schematic diagram of the results obtained for different resists [26].	14
Figure 11: Schematic diagram of photolithography and soft lithography [27].	15
Figure 12: Image of <i>Nano Spray Dryer B-90</i> [29].	16
Figure 13: Image of <i>Encapsulator B-395 Pro</i> [30].	16
Figure 14: Schematic representation of the Encapsulator B-395 Pro [32].	18
Figure 15: Image of Encapsulator B-395 Pro producing microspheres.	19
Figure 16: Results of test 2.	22
Figure 17: Results of test 3.	23
Figure 18: Main dimensions of geometry A (mm).	25
Figure 19: Main dimensions of geometry B (mm).	25
Figure 20: Main dimensions of geometry C (mm).	26
Figure 21: Schematic diagram of the main steps of the photolithography process.	27
Figure 22: Image of the structure in SU-8 obtained through an interference microscope.	28
Figure 23: Demonstrative graph of the hotplate behavior during soft-bake and PEB.	28
Figure 24: Representation of Soft Lithography [37].	30
Figure 25: Image of plasma treatment operation [38].	31
Figure 26: Image of a microdevice made by Soft Lithography.	35

Figure 27: Geometries used in this the study with different angles: 39° (A), 78° (B), 117° (C). .....	36
Figure 28: Experimental set up used in the microfluidic experiments. ....	37
Figure 29: Tracking different cells in the different channels.....	38
Figure 30: Equation to measure the deformation of RBCs [40]. ....	39
Figure 31: Results of the velocity measurements of different representative RBCs. ....	40
Figure 32: Results of the deformability measurements of different representative RBCs. ....	42
Figure 33: Deformation of cells flowing at channels with divergent bifurcations and with different angles. .....	43



# LIST OF TABLES

Table 1: Comparison of the properties and fabrication techniques between the most popular polymers for the fabrication of microfluidic devices [21]. ..... 12

Table 2: Results of the observation of the test 1 under the optical microscope. .... 20

Table 3: Properties of Newbauer Chamber. .... 22

Table 4: Information about the samples of test 2. .... 22

Table 5: Information about the samples of test 3. .... 23

Table 6: Results of the observation of the first test under the optical microscope. .... 32

Table 7: Results of the observation of the first test under the scanning electron microscope. .... 33

Table 8: Results of the observation of the second test under the optical microscope. .... 34

Table 9: Parameters used in the study. .... 37



# NOMENCLATURE

## Acronyms

RBCs	Red Blood Cells
Htc	Hematocrit
SU-8	Designation of epoxy-bored photoresist
rpm	Rotation per minute
UV	Ultraviolet
PDMS	Polydimethylsiloxane
DI	Deformation Index



# 1. INTRODUCTION

## 1.1 Objectives and Motivation

Blood is a fluid composed of a suspension of cells, proteins and ions in the plasma. In normal blood, cells occupy about 46% of their volume and these are of three different types: red blood cells (also known as erythrocytes), white blood cells (also known as leukocytes) and platelets (also known as thrombocytes). The main function of blood is to carry oxygen, nutrients and waste throughout the body. The blood flow behavior in microcirculation (comprises the smallest arteries and veins) is determined by the behavior of individual blood cells and their interactions. The cells provide the microrheological basis of flow properties of blood at macroscopic level. So in microcirculation it is fundamental to study the flow behavior at cellular level.

The manipulation of blood in vitro tests is often complex due to safety, ethical, economic and bureaucratic issues. Therefore, the development of blood-like fluids has been during the years an important research topic. Different solutions with characteristics capable of mimicking blood properties have already been achieved. However, it would be interesting to obtain a fluid which is a suspension of particles with a similar behavior of blood in the microfluidics.

The development of microfluidic devices to mimic microcirculatory phenomena has been a crucial step to understand physiological and pathological processes. Microfluidic systems are small instruments capable of working with small sample volumes, short assay times and the possibility of multiple operations.

Microfabrication technologies have become an important research area for microfluidic applications. Photolithography and micromachining in silicon were the most popular microfabrication techniques. Due to their popularity, they were adapted to the fabrication of microstructures on glass and oxidized silicon for biological and biomedical applications.

The main objectives of this master thesis are the development of a blood analogue fluid and the development and manufacture of microchannels with bifurcations to study the flow behavior of individual RBCs.

## 1.2 Structure

The present work is structured in several chapters. In the first chapter an introduction to the theme is presented, which includes the motivation and objectives, as well as their structure.

Chapter 2 presents a review of the literature on the cardiovascular system, blood properties and rheology, blood analogue fluids, and the manufacturing techniques used in this study (photolithography and soft lithography).

Chapter 3 describes the procedure used to create the blood analogue fluid, the results and the main conclusions.

Chapter 4 presents the manufacturing processes of the microdevices, the results and conclusions.

Chapter 5 presents the results obtained from the cells flowing in the fabricated microchannels (Chapter 4) and the respective conclusions.

Chapter 6 presents the final conclusions obtained after performing all the experimental activity and suggestions for future work.

Finally, the bibliographic references used for the execution of this work and the annexes are presented.

## 2. THEORETICAL FUNDAMENTALS

To understand the results that will be obtained it is important to know some important features about blood and procedures that will be used.

### 2.1 Cardiovascular system

The cardiovascular system is responsible for the transportation of materials, protection from pathogens, and regulation of the body's homeostasis. It consists of the heart, blood vessels, and the approximately 5 liters of blood that the blood vessels transport.

The heart is a muscular pumping organ, the top of the heart, known as the heart's base, connects to the great blood vessels of the body: the aorta, vena cava, pulmonary trunk, and pulmonary veins.

Blood vessels are channels that allow blood to flow quickly and efficiently from the heart to every region of the body and back again. The size of blood vessels depends of how much blood passes through the vessel. The main types of blood vessels are arteries (blood vessels that carry blood highly oxygenated away from the heart), capillaries (the smallest and thinnest of the blood vessels in the body and also the most common, they can be found running throughout almost every tissue of the body) and veins (the large return vessels of the body and act as the blood return counterparts of arteries) [1].

Blood is a non-Newtonian fluid constituted by different type of cells, platelets and a yellowish liquid called plasma. The cells present in this fluid are the Erythrocytes or Red Blood Cells (RBCs) and the Leucocytes or White blood Cells (WBCs) [2].

The figure 1 shows the composition of whole blood and it percentages.

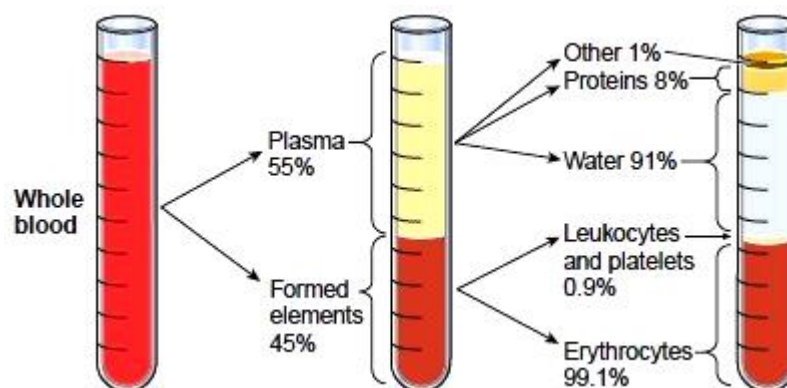


Figure 1: Composition of blood [5].

Platelets or thrombocytes are small cell fragments responsible for the clotting of blood and the formation of clots [1].

Plasma is the liquid portion of the blood and behaves as Newtonian fluid. It is a mixture of water, proteins, and dissolved substances. Around 90% of plasma is made of water, but it depends of the hydration levels of the individual [1].

Erythrocytes are cells biconcave and anucleated disc shaped of  $7\mu\text{m}$  in size. The special shape of erythrocytes gives these cells a high surface area to volume ratio and allows them to deform and pass through the thin capillaries. RBCs have two main functions: to pick up oxygen from the lungs and deliver it to tissues elsewhere and to pick up carbon dioxide from other tissues and unload it in the lungs. The cytoplasm of a RBC contains hemoglobin (Hb), gives RBCs their red color. Hemoglobin carries most of the oxygen and some of the carbon dioxide transported by the blood. They are the most common type of blood cell and make up about 45% of blood volume [1-4].

White blood cells are a very small percentage of the total number of cells in the bloodstream, but have important functions in the body's immune system [1].

## 2.2 Blood properties and flow phenomena

The Human blood is slightly alkaline and its pH lies between 7.35 and 7.45 and it is 5 times thicker than water. The high viscosity is because of the cells once plasma has a very much lower viscosity and it is affected by the change in the numbers or size of RBCs or WBCs. The viscosity is important in the sense that it determines de blood pressure [2].

### 2.2.1 Hematocrit

Hematocrit (Htc) is the proportion of blood that is made up of red blood cells by volume. The hematocrit is normally between 40% - 51% in men and 36% - 47% in women. It is usually lower in the smaller vessels in tissue than in the large veins or arteries from where the blood samples are taken [6]. When the Htc has not a value around of 45% there is some problem like Anemia, or Polycythemia (dehydration, tissue hypoxia, high altitude, blood doping in athletes), as the Figure 2 demonstrate [7].



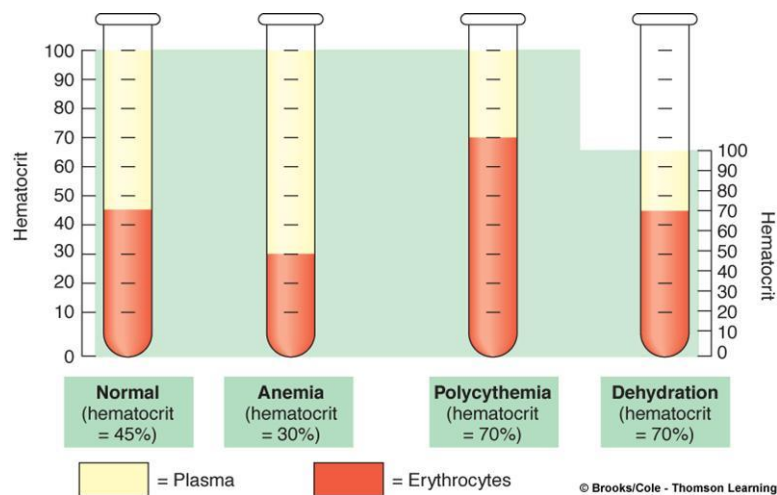


Figure 2: Hematocrit for different conditions [7].

### 2.2.2 Blood Rheology and Hemodynamics

Rheology is the scientific area that studies the flow and deformation behavior of materials. The materials can be solids or fluids, including liquids and gases. The rheological properties of blood are still being studied. They can be altered in many disease states.

Blood can be considered as a two-phase liquid, as a solid-liquid suspension with the cellular elements being the solid phase or it can also be thought as a liquid-liquid emulsion based on the liquid-like behavior of RBCs under shear.

As blood is a two-phase flow fluid liquid, its fluidity at a given shear rate and temperature is determined by the rheological properties of the plasma, cellular phases and by the hematocrit of the cellular phase.

Plasma is a Newtonian fluid, the viscosity is constant and independent of shear rate, yet technical artifacts have led some to report non-Newtonian behavior. In general, the level of plasma viscosity is a good, nonspecific indicator of disease [8].

Newtonian fluids are fluids in which the viscosity is constant for different rates of shear and does not change with time. When the viscosity varies with the rate of shear or with time, the fluid is called non-Newtonian (see figure 3) [9].

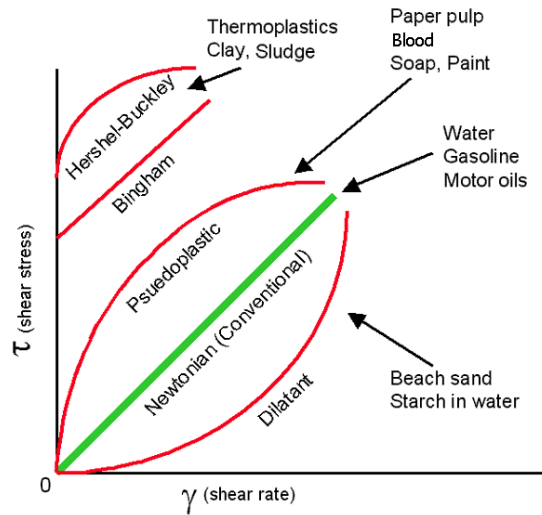


Figure 3: Newtonian and non-Newtonian fluids [10].

The concentration of cellular elements in blood determine the blood fluidity, however their rheological properties are also very important. The disturbance of flow streamlines depends not only on the concentration of blood cells but also on the behavior of them under shear forces. The major influence of this effect are RBCs, because these cells have a very special behavior.

Erythrocytes are highly deformable and tend to orient themselves with the flow streamlines, especially if the shear forces are high enough to deform these cells. RBCs have a tendency to aggregate into linear arrays, named *rouleaux*, in which they are arranged like stacks of coins and that is also an important rheological feature. The disturbance of flow streamlines becomes more notable when RBCs aggregates are formed and blood viscosity is significantly increased (see Figure 4).

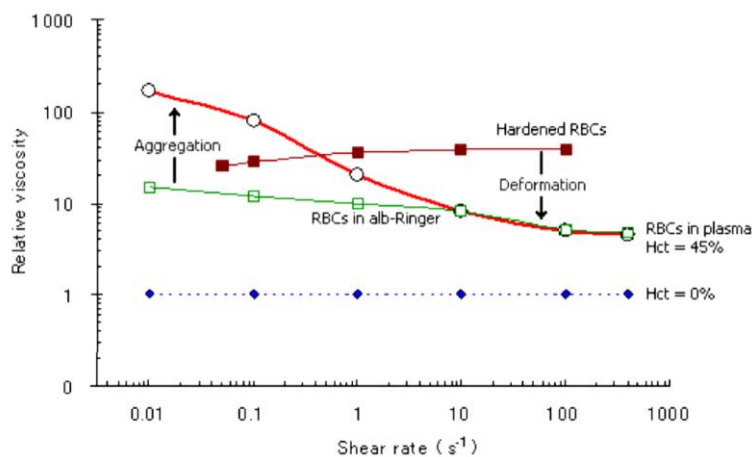


Figure 4: Relation between viscosity and shear rate of water (0% Hct), normal RBCs (45% Hct) suspended in plasma and hardened RBC's [11].

RBCs have a unique shape and structure that confer them unique mechanical properties. They respond to applied forces with extensive changes of their shape. Erythrocytes behave as elastic bodies, and thus the shape change is reversible when the deforming forces are removed. RBCs also show viscous behavior and thus respond as a viscoelastic body. Their membrane can exhibit plastic changes under some pathological circumstances and can be permanently deformed by excessive shear forces [8].

Two important factors that contribute to the RBCs properties are the viscosity determined by the hemoglobin concentration and the biconcave discoid geometry, which provides excess area for the contained volume and thus enables shape changes without increasing the surface area of the membrane [8].

The others blood cellular elements, like WBCs and platelets, have no significant effect on the macroscopic flow properties of blood but contribute to blood flow resistance and flow dynamics in the microcirculation where vessel diameters are 100  $\mu\text{m}$  or less [8].

### 2.2.3 Blood Flow behavior in Microchannels

In microcirculation the flow behavior of individual blood cells and their interactions provide the microrheological basis of flow properties of blood at a macroscopic level. Microcirculation comprises the smallest arteries and veins [12].

In large arteries, it can be adequate to consider blood as a homogeneous fluid (continuous viscous fluid). Here the Reynolds number ( $Re$ ) is large and blood flow is governed by inertial forces. However, arteries divide into successive smaller arteries and the pressure and velocity decrease as the blood flows into the smaller vessels. The  $Re$  becomes less than 1 when the blood reaches the arterioles and capillaries, where viscous force dominates over inertial forces (see Figure 5) [12].

At a microscale level it is fundamental to consider the effects of the multiphase properties of the blood on its flow behavior. A lot of phenomena happen, for example, when the microvessels are less than 300  $\mu\text{m}$ , it occurs the formation of a plasma layer, known as Fahraeus-Lindqvist. It is because of this effect that microcirculation is defined as the one including microvessels or microchannels with a diameter smaller than 300  $\mu\text{m}$  [12].

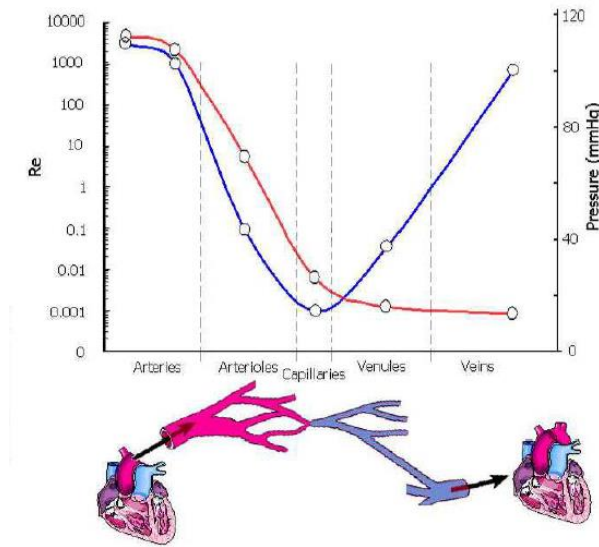


Figure 5: Schematic diagram showing the changes in blood pressure and Re on the large arteries, capillaries and veins [12].

Blood flow behavior in microcirculation is strongly influenced by the red blood cells (RBCs), since they occupy almost half of whole blood volume.

Robin Fahraeus observed that blood flow behaviors and its hematocrit (Hct) are strongly affected by microchannels with diameters less than 300  $\mu\text{m}$ . The Fahraeus effect indicates that the Hct in the glass capillaries (<300  $\mu\text{m}$ ) is lower than the feed Hct, which suggests that the Hct decreases as the blood goes through smaller microvessels. RBCs make axial migrate to the center of the microtube and consequent the motion of the cells is faster than the suspending medium. The Fahraeus-Lindqvist effect is related to this effect [12].

Fahraeus and Lindqvist observed that the apparent blood viscosity decreases as the microtube diameter became smaller (< 300  $\mu\text{m}$ ). Other works after that observed that de decrease of the apparent viscosity continues going down until diameters of about 10  $\mu\text{m}$ , but the Fahraeus-Lindqvist effect is reversed at diameters 5 to 7  $\mu\text{m}$ . This indicates that the tube Hct is not the only parameter affecting the apparent viscosity. It is believed that the plasma layer and also the microscopic motions of RBCs play an important role on the apparent blood viscosity [12].

Blood flow velocity in microvessels and microchannels has been measured during the years by several measurements techniques. Some results reported parabolic profiles, others suggested blunt profiles and even others reported blunt profiles at extremely low velocities and diameters and parabolic profiles at diameters bigger than about 100  $\mu\text{m}$ . This different results show the complexity of the phenomena happening in microcirculation. However, it is clear that the flow velocity profiles are strongly affected by several parameters as: Hct, microtube diameter, shear rate, flow rate, suspension fluid, experimental

errors, concentration of trace particles, etc. Despite the great amount of research on this area controversies still remain [12].

The Zweifach-Fung or bifurcation effect is a well known phenomenon in microcirculation. It reports that in a bifurcation the child branch with the lower flow rate is depleted in RBCs as compared to the parent vessel, while the other child branch, with higher flow rate is enriched with cells (see figure 6). When the flow rate is sufficiently small, the hematocrit in the child branch can even drop down to zero, while it reaches high values in the other branch [13].

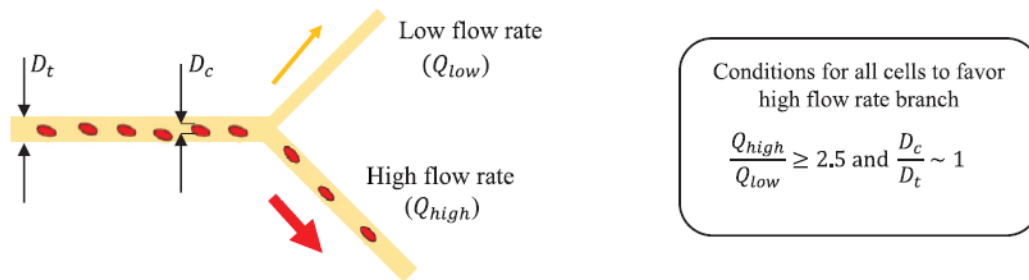


Figure 6: Separation of the cells in the bifurcations [14].

Another phenomenon that has been investigated is the phase separation at single bifurcations. This may be influenced by the feed hematocrit, channel geometry and flow rate distribution [14].

Recently a research study has revealed that hematocrit partition can be completely reversed, which means that the low flow rate child branch can be enriched in RBCs compared to the parent vessel. This phenomenon was observed at low hematocrit (5%). For such low hematocrit the RBCs partition at the level of bifurcations depends strongly on the viscosity contrast between the viscosities of the RBC hemoglobin and the suspending fluid (see figure 7) [13].

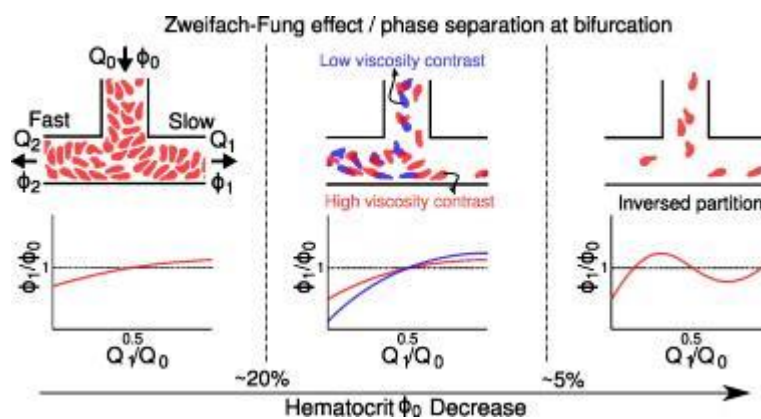


Figure 7: Scheme showing the influence of the hematocrit on the separation phase of RBCs. [13].

## 2.3 Blood analogue fluids

Using blood in experimental studies is not always practical mostly due to safety reasons, so the developing of a viscoelastic fluid with rheological characteristics similar to human blood has gain importance as a safe alternative.

Different combinations have been done for this purpose as blood analogue solutions made from high molecular weight polymers dissolved in water, namely aqueous solutions of polyacrylamide and xanthan gum at different concentrations. The polyacrylamide and xanthan gum solutions have a rheological behavior similar to the human blood behavior at concentrations of 125 and 500 ppm, respectively, especially at low shear rates [15].

Other studies were performed with Newtonian blood analogues composed of mixtures of glycerol and water, but they do not work at microfluidic scale level.

Successful blood analogue were developed based on sucrose and dimethylsulfoxide with xanthan gum by Campo-Deaño et al. [16]. They had viscosity curves and viscoelastic moduli similar to whole human blood and it was demonstrated that these analogues can be used in PDMS microfluidic devices due to their refractive index matching. However, it is crucial to take into account the blood elements, especially when in vitro flow studies intend to investigate microcirculation phenomena occurring at hematocrits of about 20%-25% [17].

Currently, there are still few works about particulate blood analogue fluids, that is, a base fluid containing solid suspended elements. However, none of them are capable of mimicking the blood element behavior. It was developed a blood analogue made by a Newtonian solvent containing a suspension of microcapsules and then using a non-Newtonian solvent that is capable to reproduce the steady viscosity, but they did not study any microscale flow phenomenon [17, 18].

In a study performed by Calejo et al [19], their results showed that the cell free layer originated from the particles depends strongly on the base fluid, but developments and improvements are needed to mimic blood flow phenomena occurring at the microcirculation level (see figure 8).

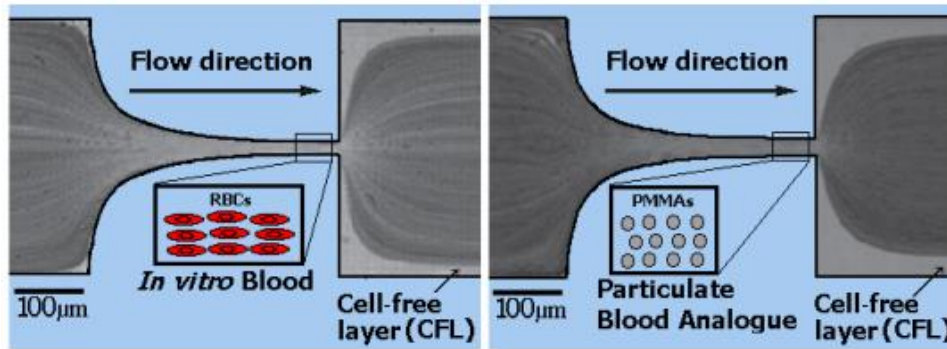


Figure 8: Flow of Red Blood Cells (left side) and blood analogue fluid with PMMA particles (right side) through a hyperbolic microchannel [19].

## 2.4 Microfabrication of biomedical microdevices

Microfabrication technologies have become an important research area for microfluidic applications in the last 20 years. These applications cover different scientific and industrial areas as environment, pharmaceuticals or biomedical engineering [20].

Biomedical microsystem technologies for diagnosis applications have an extremely enhanced potential for being used as point-of-care devices. Usually they feature high analytical performance, high system-integration, improved potential for automation and control, small volume of analyses and reagents, safety, reduced cost, greater sensitivity, disposability and shorter analysis times, when compared to the conventional size systems [20].

In 1990 Manz et al. proposed the first miniaturized analysis system (TAS). It was able to automatically perform the sampling, transport, chromatographic separations and detection of samples at a microscale level. After that, many researchers have proposed micrototal analysis systems for different applications and have explored different microfabrication techniques [20].

Photolithography and micromachining in silicon were the most popular microfabrication techniques in the 90s decade, because of their vast use for microelectronics integrated circuits and microelectromechanical systems (MEMS). Due their popularity, they were adapted to the fabrication of microstructures on glass and oxidized silicon for biological and biomedical applications [20].

Silicon is optically opaque and semiconductor and, consequently, inappropriate for certain types of separation and detection mechanisms. These limitations led to the research of alternative materials, so polymers started to be used for microfluidic structures fabrications. They emerged as an attractive alternative to glass and silicon, due to their low-cost, wide range of mechanical and chemical properties, flexibility and easy processing and because the fabrication process is based on replication, which makes this process faster and less expensive [20].

The most popular polymers for microfluidic systems are poly(dimethylsiloxane) (PDMS), poly(methylmethacrylate) (PMMA), high-density polyethylene (HDPE), low-density polyethylene (LDPE), polyamide 6 and SU-8 (see table 1) [20, 21].

Table 1: Comparison of the properties and fabrication techniques between the most popular polymers for the fabrication of microfluidic devices [21].

Polymer	Main characteristics	Fabrication techniques
<b>PMMA</b>	Thermoplastic. Transparent. UV resistance. Low water absorption. Good abrasion resistance.	Injection moulding. Hot embossing. Laser photoablation. X-ray lithography.
<b>COC</b>	Thermoplastic with high transparency. High heat resistance. Low water absorption. High stiffness and strength.	Injection moulding. Hot embossing.
<b>PS</b>	Thermoplastic. Excellent electrical properties. Resistant to a wide variety of chemicals.	Injection moulding. Hot embossing. Laser photoablation.
<b>PC</b>	Transparent thermoplastic. High heat resistance. High stiffness and strength.	Injection moulding. Hot embossing. Laser photoablation.
<b>PTEG</b>	Transparent thermoplastic. Good impact and chemical resistance.	Hot embossing. Laser photoablation.
<b>PDMS</b>	Transparent elastomeric polymer. Biocompatibility. High flexibility. High gas permeability. UV resistance. Chemically inert. Thermally stable.	Soft-lithography. Direct laser plotting.

#### 2.4.1 Photolithography

Photolithography is a highly developed technology for micropatterning and microfabrication and to use it is needed a mask and a layer which is sensitive to light. The main goal of this optical lithography is to transfer the opaque pattern from the mask to the photosensitive layer, the photoresist [20, 22].

To create a mask, first it has to be designed with a computer-aided design (CAD) software, often in AutoCAD or other suitable software packages such as L-Edit, and it is important that the software can handle various zoom ranges, because the structures often includes patterns on the order of microns.



The data is sent to the manufacturer and then processed into internal CAD format (Gerber) and transferred to a lithography tool which then exposes the design onto the photomask substrate. The equipment and exposure process used can be the same for both glass and film photomasks. Once the manufacturing process is finished, the mask is cleaned and inspected, ready to be shipped to the laboratory for fabrication of microfluidic molds [22, 23].

Usually, in small structures, photoresists are applied using spin coating or spraying and, although some of them are applied as films which are laminated onto the substrate, the spun-on photoresists are the most popular. Spin-on photoresists contain an organic solvent which dissolves the resin and radiation sensitive compound. The conformity and uniformity of the films depends on the details of the spinning procedure (see figure 9).

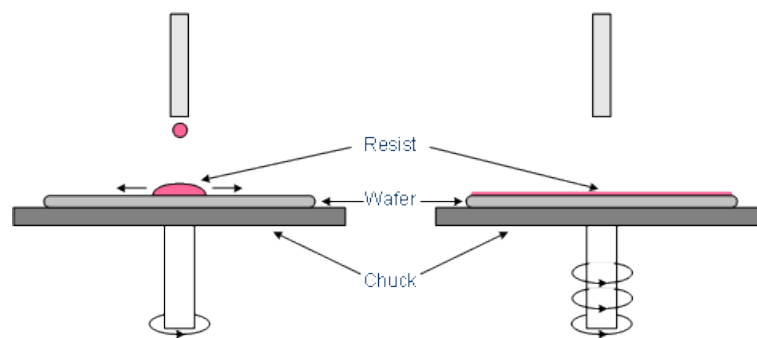


Figure 9: Scheme of spinning [25].

The photoresists are polymers, and they are sensitive to light of particular wavelengths, so when exposed their chemical structure changes. Usually they are sensitive to UV light with the i-line of mercury (365 nm) being especially popular [22]. To make the exposure it is possible to use three different methods as light source: Mask-Aligner, Stepper and Laser beam [24].

The pattern is developed in the photoresist after the exposure to light and for that it is used a suitable developer. The developer can be an alkaline solution (such as Tetramethylammonium hydroxide – TMAH) or an organic solvent (such as Propylene glycol methyl ether acetate – PGMEA).

After exposure some photoresists become more soluble, and it is called positive tone photoresists, while others become less soluble and they are called negative tone photoresist like SU-8. A third kind of photoresist is the image-reversal photoresist. This type of resist is basically a positive photoresist, but after light exposure, the resist is subjected to an image reversal process by which the exposed areas become insoluble and the unexposed areas become soluble [22]. It is possible to see how they work in the figure 10.

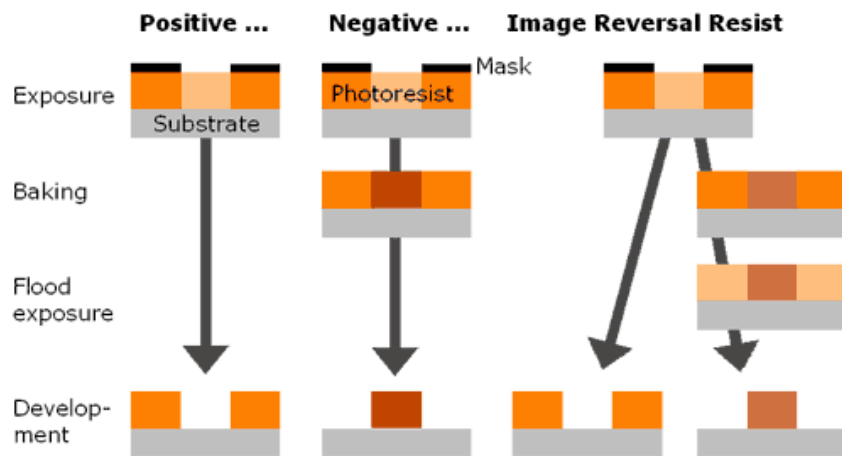


Figure 10: Schematic diagram of the results obtained for different resists [26].

SU-8 photoresist has received a lot of attention in recent years. Due to their combined material properties, it has been at the core of many devices and processes. SU-8 offers good chemical and mechanical stability, ease of patterning and possibility of high-aspect ratio structures. Processing of SU-8 involves: spinning, softbake (solvent removal), exposure, post exposure bake (PEB) and development in organic solvent. Cross-linking mainly takes place during the post exposure bake [22].

#### 2.4.2 Soft lithography

Soft lithography is a simple process that allows to product microstructures in a rapidly way, as the figure 11 shows. This technique is often used in laboratories for fast production of moderate numbers of prototypes and the sizes of the structure depend mainly on the quality of the mold.

Soft lithography uses chemicals processes to harden the polymer, usually, a base (as PDMS) and a hardener or cure, are mixed just prior to use. The chemical cure process starts immediately upon mixing the two components and after a while, results in the hardening of the polymer. The mixture is leaked in the mold and as the polymer sets the polymer takes the shape of the mold. After being baked, the polymer structure can be removed from the mold [22].

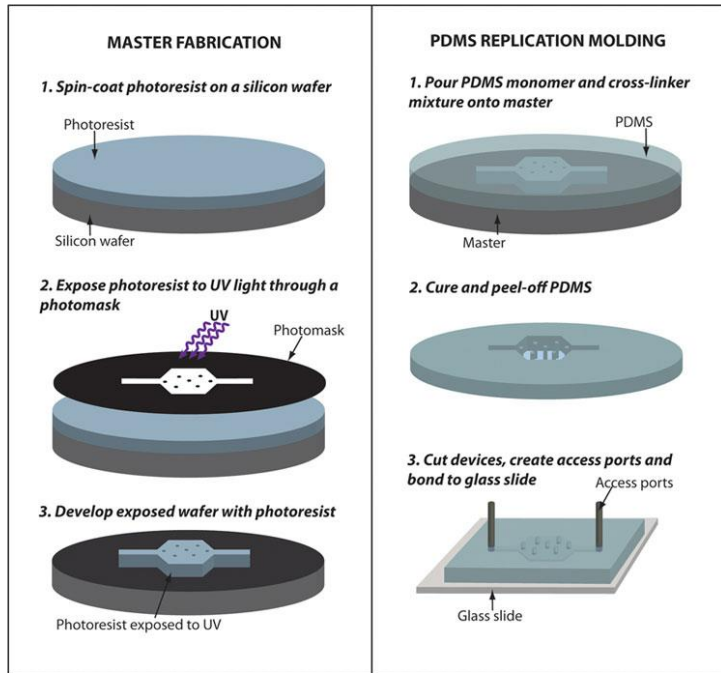


Figure 11: Schematic diagram of photolithography and soft lithography [27].

### 3. DEVELOPMENT OF A BLOOD ANALOGUE FLUID

The human blood is a complex fluid that carries vital substances. A characterization of blood rheology and its flow dynamics is very important in order to predict cardiovascular diseases, to understand the transport of drugs through the circulatory system, and for the development of new equipment as blood pumps. However, the handling of blood is not a simple task and may not always be practical due to safety reasons. Due to this, blood analogue fluids are frequently used for in vitro experiments because they have several advantageous characteristics as nontoxicity, low cost, and transparency [28].

The blood rheology is extremely complex, so it is difficult to develop analogue fluids that have all the rheological properties of blood. The purpose of this study is to produce a blood analogue fluid having as its main focus on the particulate matter of the blood, i. e., the red blood cells (they represent 45% of the blood) that have a critical influence on the blood flow properties at a microscale level [28].

#### 3.1 Materials and Methods

To create the blood analogue fluid it was attempted to mimic the red blood cells in size and deformability by producing flexible microspheres. Two different techniques were tested: the *Nano Spray Dryer B-90* (Figure 12) and the *Encapsulator B-395 Pro* (Figure 13).



Figure 12: Image of *Nano Spray Dryer B-90* [29].



Figure 13: Image of *Encapsulator B-395 Pro* [30].

The Nano Spray Dryer B-90 was designed to produce particles out of a solution or suspension with a particle size between  $0.3\ \mu\text{m}$ – $5\ \mu\text{m}$ . The sample material is dried by a hot gas [31].

The Encapsulator B-395 Pro is a versatile system for controlled encapsulation of active ingredients. It allows the production of monodisperse microbeads and microcapsules and it is possible to choose diameters between 80  $\mu\text{m}$  and 4000  $\mu\text{m}$  [32].

In both equipment it is possible to adjust the procedures and obtain particles with sizes outside the ranges mentioned. However, the equipment used was the Encapsulator B-395 Pro because it is easier to handle, faster to produce and has a better yield.

The bead size is controlled by several parameters as vibration frequency, nozzle size, flow rate, and physical properties of the used material.

The material used for the manufacture of microspheres was alginate. It is a naturally occurring anionic polymer typically obtained from brown algae (Phaeophyceae) [33].

Alginate is a biomaterial that has numerous applications in the field of biomedical due to its properties such as biocompatibility, low toxicity, relatively low cost and ease of gelation by addition of divalent cations such as  $\text{Ca}^{2+}$  [33].

The most common way to prepare hydrogels from an aqueous alginate solution is to combine the solution with ionic crosslinking agents such as divalent cations [33].

In this work, to obtain the alginate hydrogel microspheres, Calcium Chloride ( $\text{CaCl}_2$ ) was used as the crosslinking agent.

Through the figure 14 it is possible to visualize the process of formation of the microspheres.

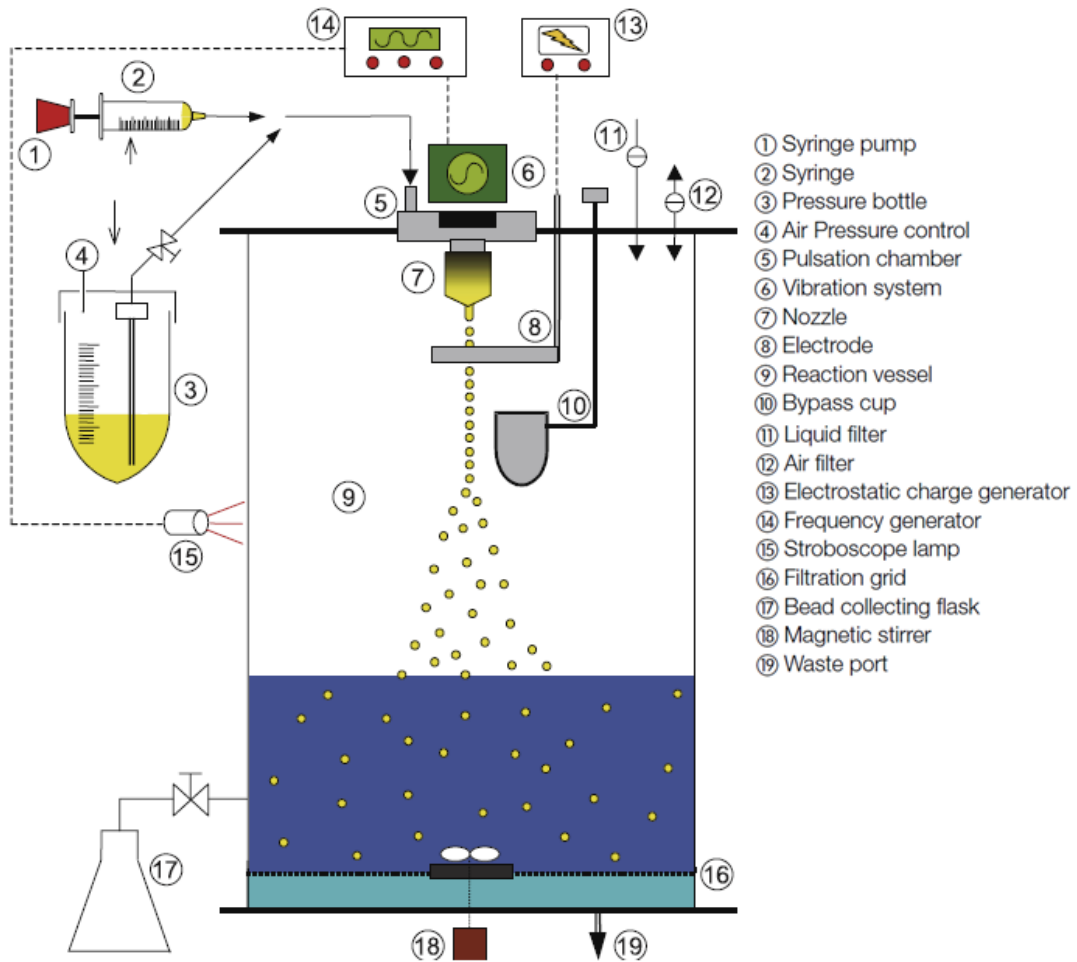


Figure 14: Schematic representation of the Encapsulator B-395 Pro [32].

The alginate is put into a syringe (2). The polymer is forced into the pulsation chamber (5) by a syringe pump. The liquid then passes through a precisely drilled nozzle (7) and separates into equal size droplets on exiting the nozzle. These droplets pass through an electrical field between the nozzle (7) and the electrode (8) resulting in a surface charge. Electrostatic repulsion forces disperse the beads as they drop to the hardening solution ( $\text{CaCl}_2$ ). Optimal parameters for bead formation are indicated by visualization of real-time bead formation in the light of a stroboscope lamp (15). When optimal parameters are reached, a standing chain of droplets is clearly visible. Once established, the optimal parameters can be preset for subsequent bead production runs with the same material. Poorly formed beads, which occur at the beginning and end of production runs, are intercepted by the bypass cup (10). Depending on several variables, 50 to 5000 beads are generated per second and collected in a hardening solution within the reaction vessel (9). Solutions in the reaction vessel are continuously mixed by a magnetic stir bar (18) to prevent bead clumping [32].

Figure 15 shows the *Encapsulator B-395 Pro* at a time when it was producing microspheres. The amount of hardening solution should be about 10 times more than the amount of Alginate. In each procedure 10 ml of Alginate and 100 ml of the hardening solution were used. The concentration of Alginate used was 2% (the alginate was diluted with water). Different concentrations of Calcium Chloride (hardening solution) and different values of frequency were tested. Interesting results were also obtained when using a surfactant (TWEEN 80) mixed with Calcium Chloride. All samples were filtered with a porous filter 40  $\mu\text{m}$  in order to eliminate the larger ones.



Figure 15: Image of Encapsulator B-395 Pro producing microspheres.

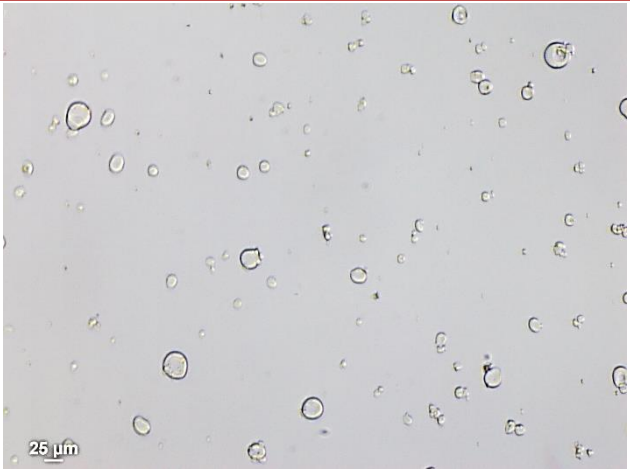
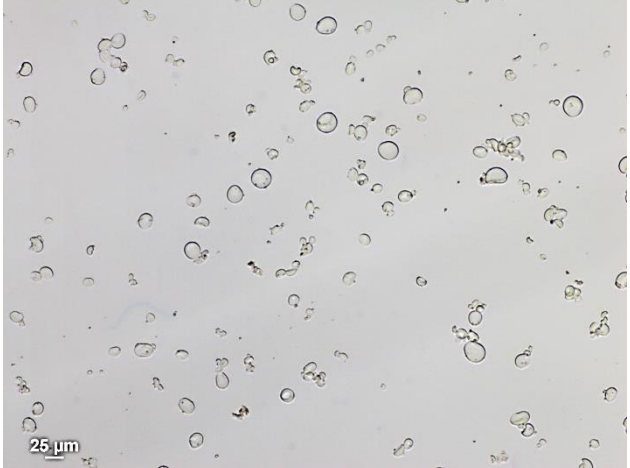
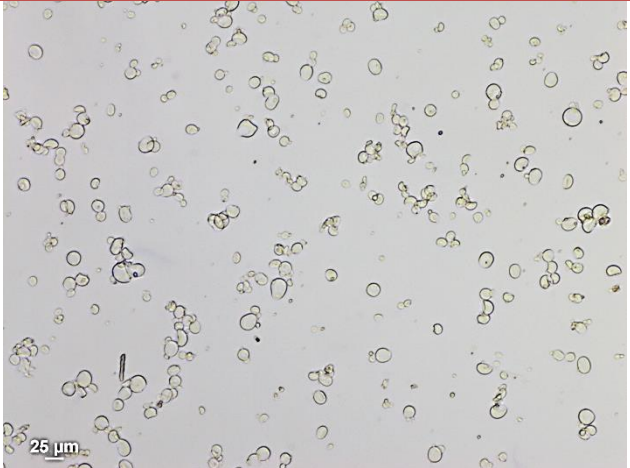
## 3.2 Presentation and discussion of results

By using an Encapsulator B-395 Pro, different tests were performed to obtain the best protocol.

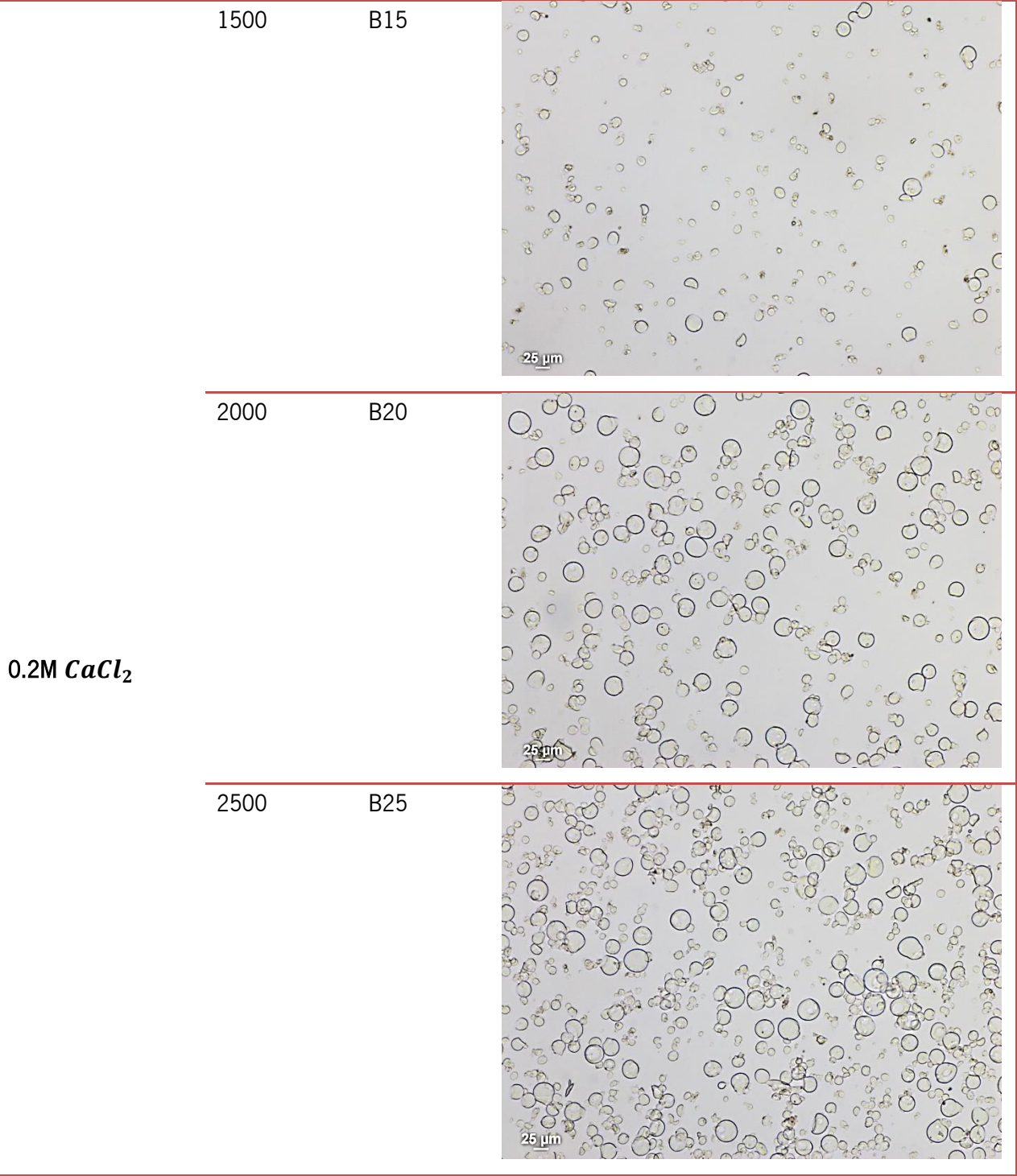
### 3.2.1 Test 1

Three solutions of Calcium Chloride with a concentration of 0.1M and three solutions with a concentration of 0.2M were prepared. Three different frequency values were tested for each concentration. The results are in table 1.

Table 2: Results of the observation of the test 1 under the optical microscope.

Concentration (Mol)	Frequency (Hz)	Sample name	Microspheres observed in a optical microscope
0.1M $CaCl_2$	1500	A15	 Micrograph showing numerous small, spherical microspheres of varying sizes. A scale bar in the bottom left corner indicates 25 μm.
	2000	A20	 Micrograph showing a higher density of microspheres compared to the 1500 Hz sample. A scale bar in the bottom left corner indicates 25 μm.
	2500	A25	 Micrograph showing a very high density of microspheres, with many overlapping. A scale bar in the bottom left corner indicates 25 μm.





It is possible to see that the number of spheres increases when the concentration of Calcium Chloride is 0.2 M and when the frequency is 2500 Hz. Therefore, the sample with the greatest amount of particles is B25.

### 3.2.2 Test 2

In order to avoid aggregation of beads, TWEEN 80 was added to the Calcium Chloride solution. The frequency of 3000 Hz (maximum frequency of the equipment) was also tested to compare with the sample B25.

In order to obtain more concrete results a Neubauer Chamber was used for counting the particles. The characteristics of the Neubauer Chamber are in table 3.

Table 3: Properties of Neubauer Chamber.

Depth	100 $\mu\text{m}$
Area	0.0025 $\text{m}^2$
Volume	0.00025 $\text{mm}^3 = 0.00025 \mu\text{l}$

Table 4 shows the samples from which the results were obtained and in figure 16 it is possible to see the results.

Table 4: Information about the samples of test 2.

Solution	Frequency (Hz)	Sample name
0.2M $\text{CaCl}_2$	2500	B25
0.2M $\text{CaCl}_2$ + TWEEN 80 (0.1%)	2500	S25
	3000	S30

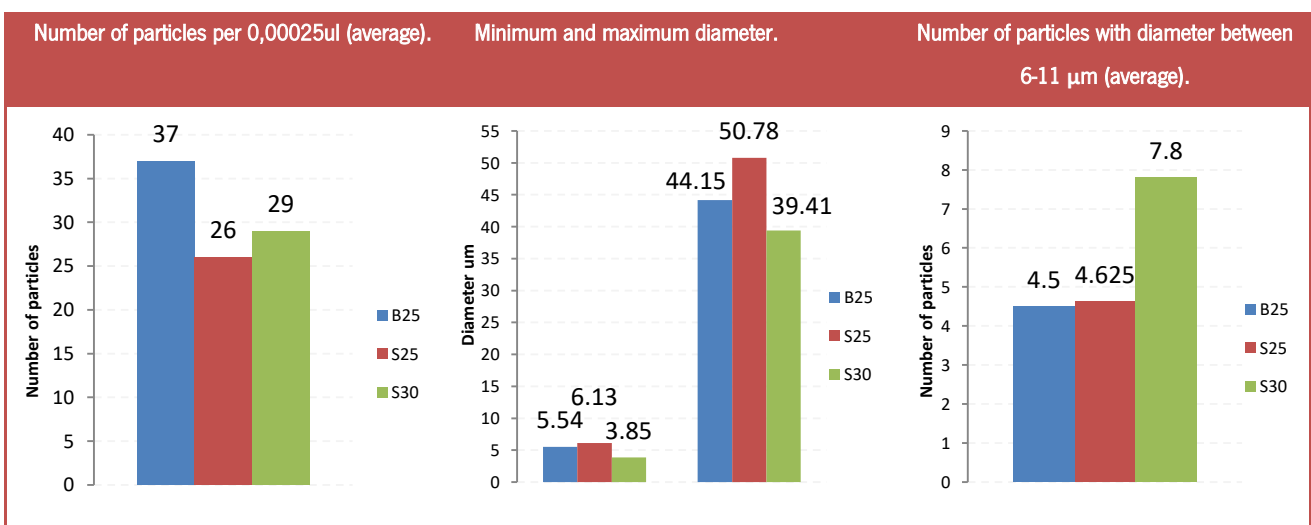


Figure 16: Results of test 2.

The frequency 3000 Hz leads to a higher production of microspheres, however the surfactant causes the quantity to decrease. Apparently the surfactant also leads to a smaller bead production since the sample B25 and S25 have different amounts in total but the same amount of spheres having the diameter in the range 6-11  $\mu\text{m}$ .

### 3.2.3 Test 3

In this test different percentages of TWEEN 80 were tested. In the table 5 are the solutions prepared and in figure 17 the results of the samples.

Table 5: Information about the samples of test 3.

Solution	Frequency (Hz)	Sample name
<b>0.2M <math>\text{CaCl}_2</math> +</b>	TWEEN 80 (0.05%)	T05
	TWEEN 80 (0.1%)	T1
	TWEEN 80 (0.2%)	T2
	TWEEN 80 (0.5%)	T5

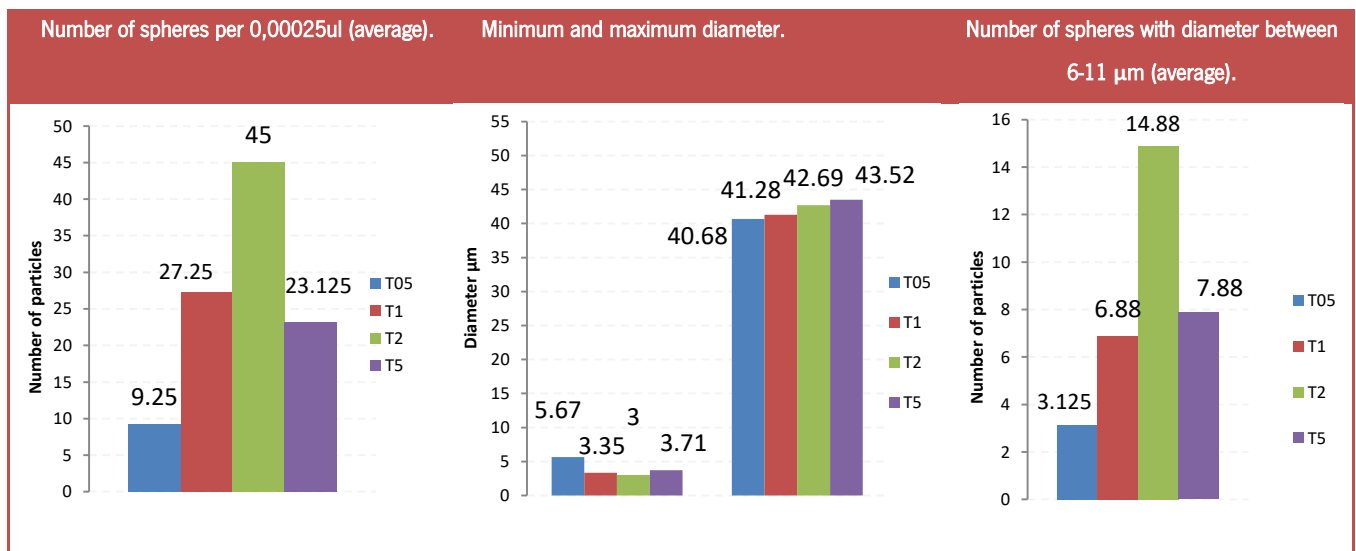


Figure 17: Results of test 3.

The amount of beads increases up to the percentage of 0.2% of TWEEN 80 as well as the number of beads with a diameter between 6-11  $\mu\text{m}$ .

### 3.3 Conclusions

Our results allow us to conclude that this method has potential to production of microparticles able to mimic RBCs. From our results, it is possible to conclude that the ideal composition for the hardening the solution is 0.2M Calcium Chloride and 0.2% TWENN 80 (the increase of the surfactant TWENN 80 to 0.2% led to an increase in the number of spheres with the size of interest.). In addition, it was concluded that the best frequency is 3000 Hz, which allow us to produce in a few minutes about  $5.952 \times 10^9$  of microparticles.

## 4. FABRICATION OF MICROCHANNELS WITH DIVERGING BIFURCATIONS

The fabrication of the microchannels starts with drawing the geometries using AutoCAD. The geometries created were based in a previous work performed by Campos [34]. The objective of these geometries is to evaluate the flow behavior of the red blood cells in bifurcations with different geometries.

The geometry A represented in the figure 18 is the starting point of the geometries tested in present work.

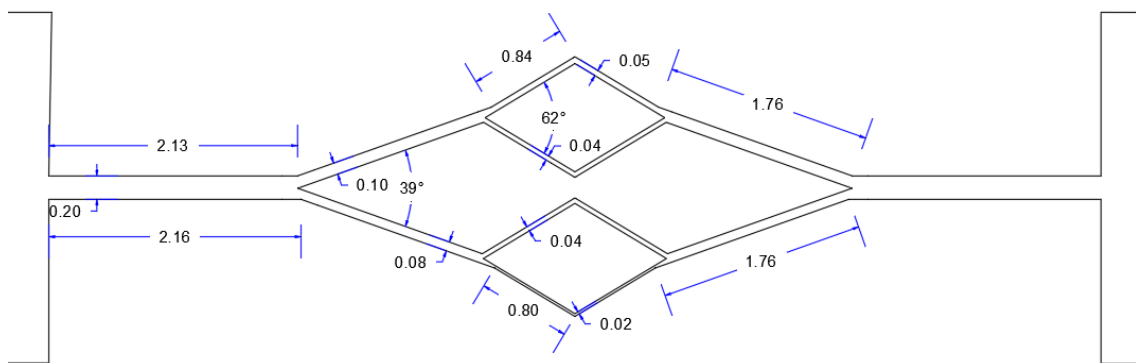


Figure 18: Main dimensions of geometry A (mm).

In the figure 19 it is possible to see the main dimensions of geometry B. The only difference between the geometry A and B is the angle of the first divergent bifurcation that is the double.

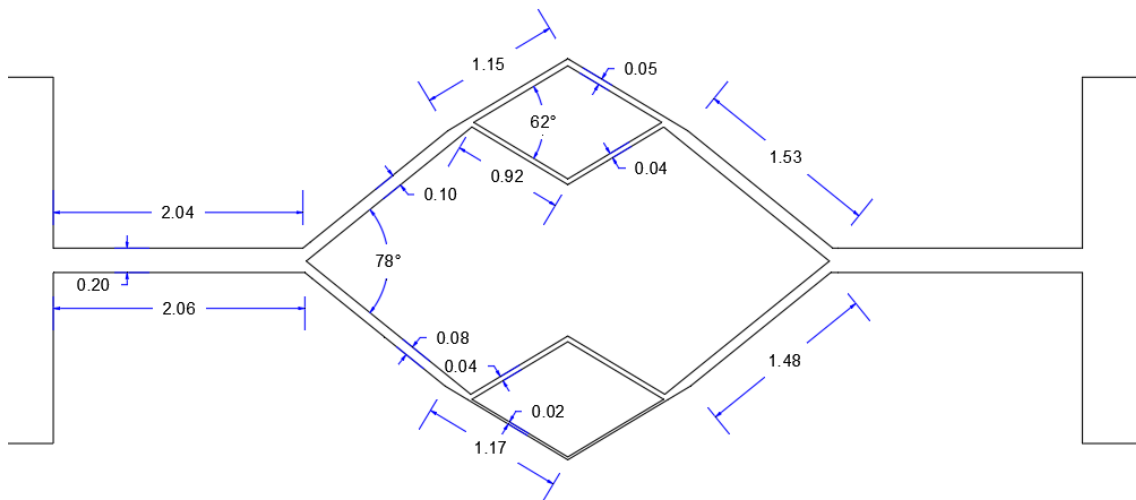


Figure 19: Main dimensions of geometry B (mm).

The figure 20 shows the main dimensions of geometry C that is similar to geometry A but the first angle is 3 times bigger.

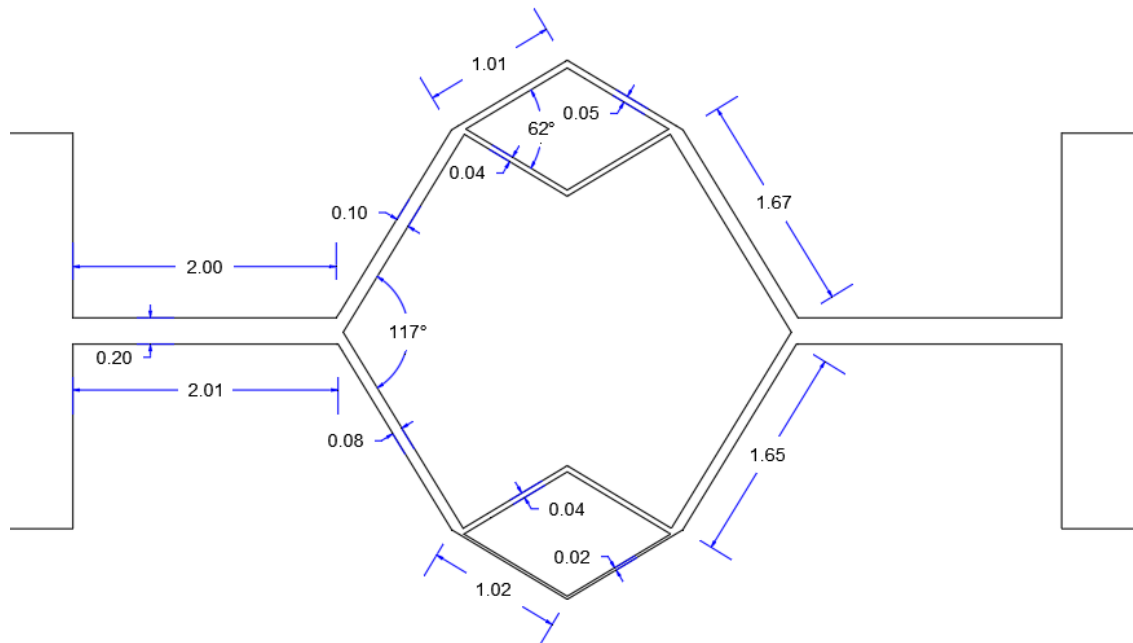


Figure 20: Main dimensions of geometry C (mm).

## 4.1 Materials and Methods

The techniques used to produce the microfluidic devices were the photolithography and soft-lithography.

### 4.1.1 Photolithography

All geometries were printed in a film mask to be used at photolithography process. The photoresist used was SU-8 2025 which has a datasheet with the protocol that should be followed. However, the SU-8 properties change over the time and as a consequence most of the times the results are not the expected ones, so it is frequent to make some adjustments to the protocol suggested by the manufacture. When the SU-8 is not used for a period it is necessary to make some preliminary tests before using it again otherwise the results will not correspond to what is expected. The wafers used in this work were made of silicon or glass. Additionally, it was added a chromium layer in all of them to increase the adherence of the SU-8.

The main steps of the photolithography process used in this work are shown in figure 21.



Figure 21: Schematic diagram of the main steps of the photolithography process.

Before starting the photolithography process it is important to clean and remove the water from the surface of the wafer. Hence, the wafer needs to be heated in an oven at 200°C for about 10 minutes.

Note that, it is important to change the light from white light to yellow in clean rooms. The fluorescent light consists of glass tubes that contain gases and one of them is mercury [35]. The mercury g-line (365 nm) is used in the exposure of the SU-8 so the light used in clean rooms has to be changed to a color that does not contain mercury.

### SU-8 coat

The wafer is placed at the center of a machine called spin coater. A small amount of SU-8 similar to a 2 euro coin is poured into the center of the wafer. The height of the channels will depend on this step as it is determined by the speed of rotation of the spin coating. In all situations, the *SU8 25 100* program was used which has reached a maximum rotation of 2000 rpm and therefore all the structures had a height of about 30 micrometers (as shown in figure 22).

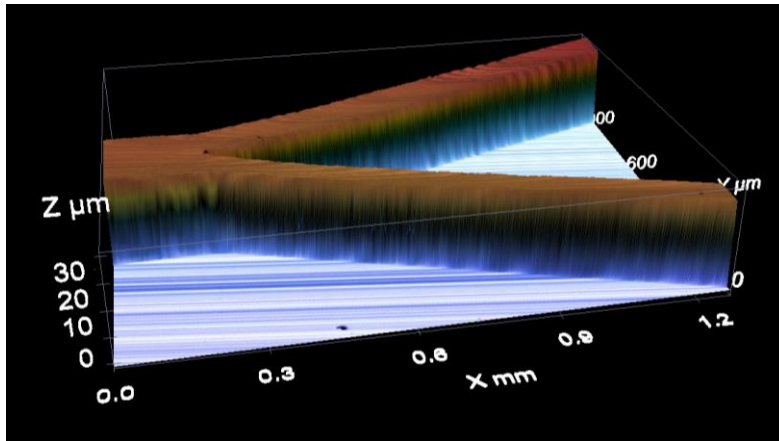


Figure 22: Image of the structure in SU-8 obtained through an interference microscope.

### Soft-Bake

This step is made to remove the SU-8 solvent and make it more solid. Most of the solvent evaporates changing the thickness of the layer and preparing the photoresist to be exposed [36].

To make the soft-bake it is needed a hotplate. This machine allows a controlled bake and the process is represented in figure 23. The temperature increases really fast since the room temperature until 40°C (about 1 minute) then it raises 2°C/minute. When it reaches 65°C the hotplate keeps that temperature for 5 minutes and the same procedure happens when it reaches 95°C but for 10 minutes. The hotplate was programmed to make these ramps, to not induce stress on the structures (stress happens when the heating is too fast).

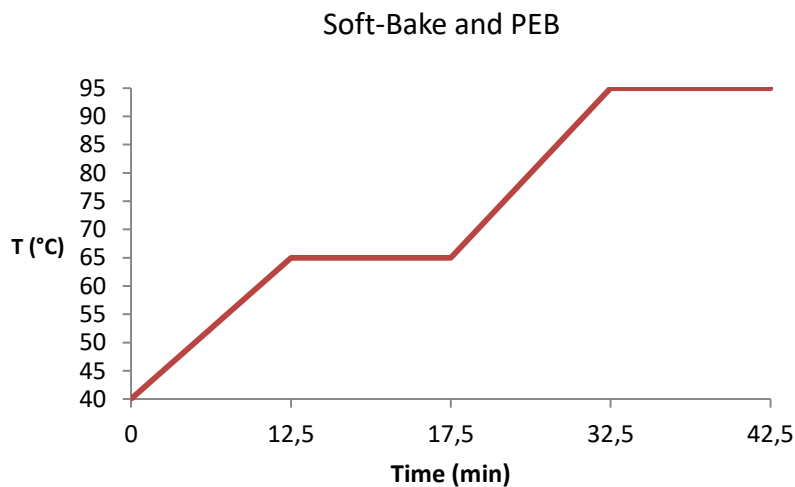


Figure 23: Demonstrative graph of the hotplate behavior during soft-bake and PEB.



After finishing the soft-bake process the wafer is removed from the hotplate and its left to cool down to room temperature for 10 minutes.

### SU-8 exposure

The SU-8 substrate is exposed to UV light and the cross link starts. The film mask is placed on the top of the wafer allowing the radiation to reach only some specific areas (the geometry).

The datasheet provides the information about the energy that should be used in the substrate depending on the material of the wafer and the thickness of the coat. In this case the ideal is between 225 and 300 mJ/cm<sup>2</sup> due to the chromium layer.

To make the exposure it is possible to use different radiation sources. In this case it was used a mask aligner machine, not because of the alignment function, but because it was the radiation source available in the laboratory. The machine's lamp provides uniform radiation and collimated light and therefore a good exposure process.

To define how much time the photoresist should be exposed it was needed to determine the energy that the machine provides per second. The elements parts were all positioned and the result was 1.9 mJ/cm<sup>2</sup> per second. The elements are: the film mask, two glasses (to make pressure and reduce the distance between the mask and the wafer) and a filter to eliminate UV radiation with wavelength below 350 nm (radiation with a wavelength below 350 nm has a lot of energy and immediately begin the cross-linking in the surface of the structure not allowing the radiation to reach the whole structure so it is not possible to obtain vertical sidewalls in the SU-8). After that, the value found was between 119 and 158 seconds. This step is very important and determinant for the quality of the structures. So several tests have been done and the main results are shown in the section below.

### Post Exposure Bake (PEB)

The Post Exposure Bake accelerates the cross-linking of the exposed areas making them insoluble in the developer. This step is made the same way as soft-bake but instead of removing the wafer from the hotplate to let it cool down, the wafer cools down slowly in the hotplate to remove the stress and avoid cracks.

## SU-8 development

This step is intended to remove the SU-8 that has not been cross-linked. The wafer is immersed in developer for about 10 minutes. The structures should not have white parts (the white parts are SU-8 not exposed that must be removed or SU-8 that needs more exposure).

## Rinse and Dry

After the development the wafer is rinsed with Isopropanol. This procedure must be done in just a few seconds because the SU-8 can be released from the wafer. To dry it is used compressed air.

### 4.1.2 Soft lithography

Through soft lithography it is possible to produce several microdevices quickly and economically. The microdevices are produced in PDMS using the master constructed in photolithography.

In a container the PDMS and the curing agent are mixed in proportions of 10: 1 respectively. The degassing process is then carried out by placing the mixture in vacuum. The SU-8 master is placed in a petri dish, the mixture is poured over the master and degassed in the vacuum pump. The petri dish is placed in the oven at 80°C for 20 minutes. Finally the PDMS is removed from the mold (figure 24).

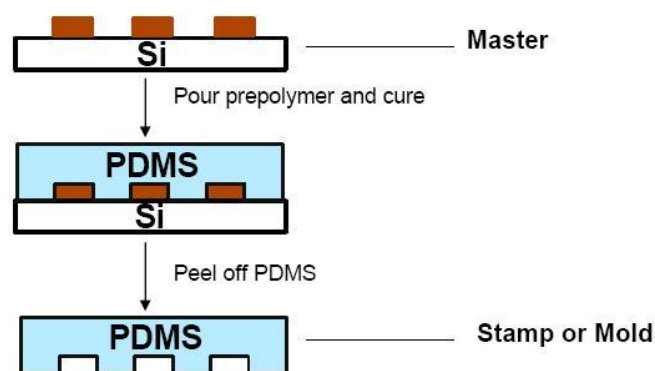


Figure 24: Representation of Soft Lithography [37].

Plasma treatment is used to close the channels. The PDMS and a glass slide are treated in an O<sub>2</sub>-plasma and it cleans the surface and activates them by cracking bondings and creating reactive sites (figure 25). So it is possible to get a strong bonding of the surfaces [38].

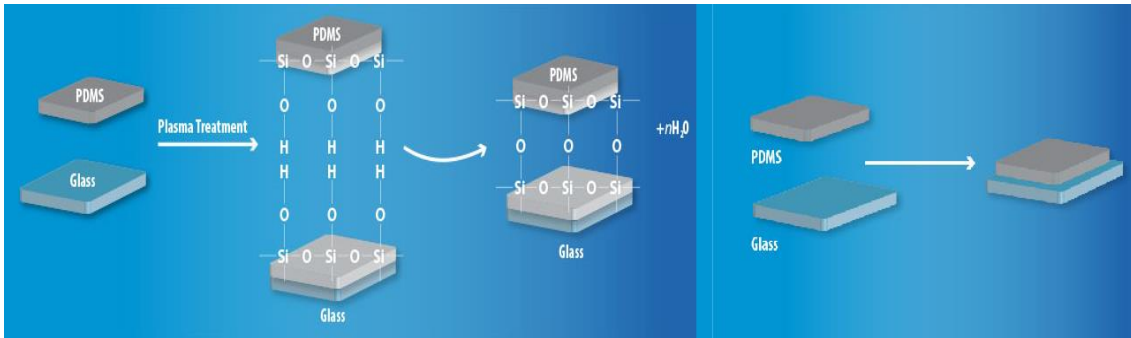


Figure 25: Image of plasma treatment operation [38].

## 4.2 Results and Discussion

### 4.2.1 Photolithography

In this work several tests were performed to determine the best exposure time. The cleanroom temperature ( $23^{\circ}\text{C} \pm 2$ ) was always identical in all tests, so the properties of SU-8 were the same for all tests.

#### Test 1

In this test 3 different exposures were tested by using the same geometry and the results are in table 6 and table 7.

Table 6: Results of the observation of the first test under the optical microscope.


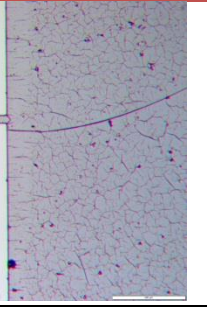
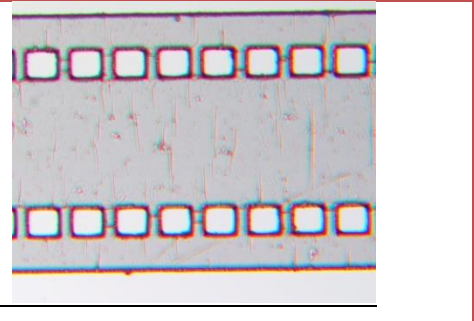
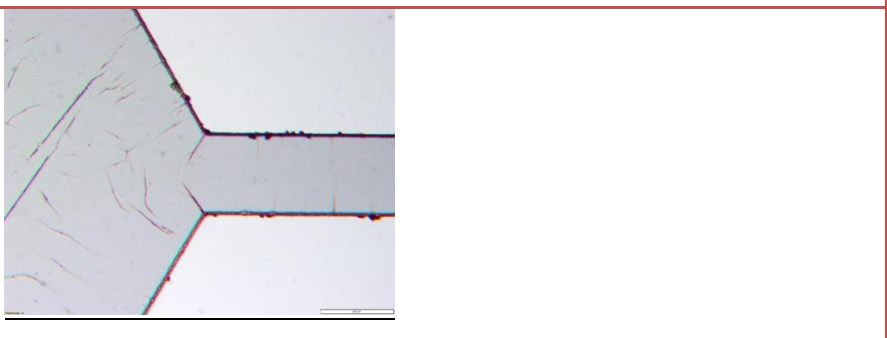
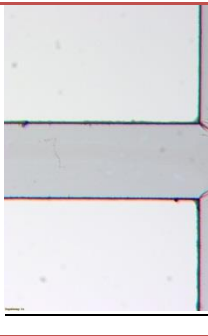
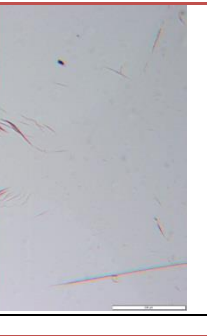
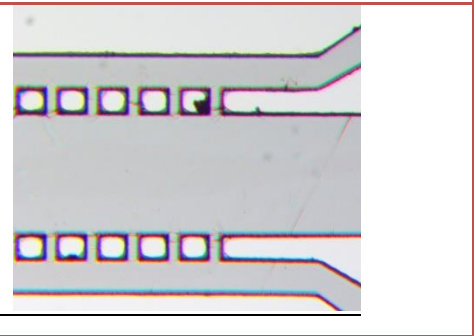
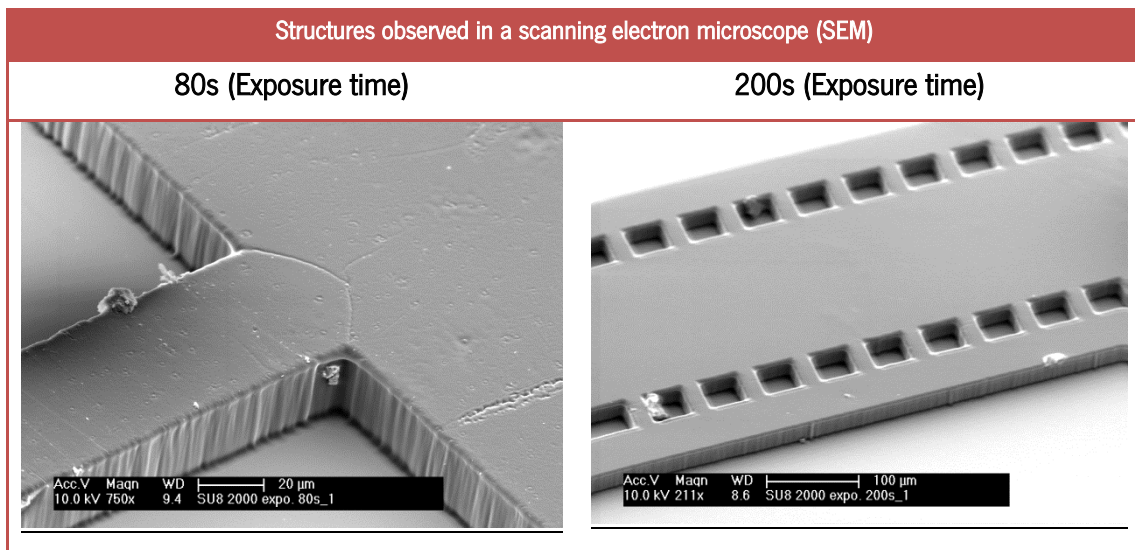
Exposure time (s)	Structures observed in a optical microscope		
80			
100			
200			

Table 7: Results of the observation of the first test under the scanning electron microscope.

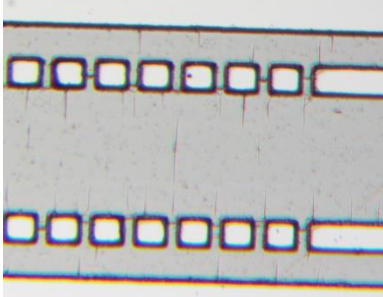
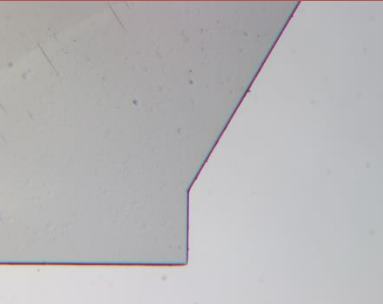
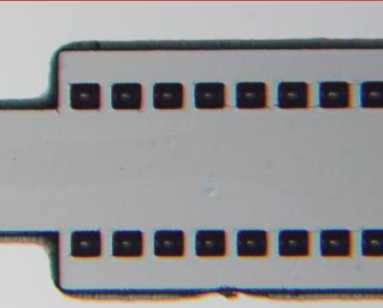


The results show that by increasing the exposure time, the cracks in the SU-8 structure decrease. Comparing the exposure time of 80s and 200s it is clear that this parameter influences the definition of smaller structures. In addition, it is possible to observe that the cracks are superficial and do not reach the entire structure, which means that the structure is not damaged and cracks are only scratches.

## Test 2

In this test the exposure times 100s, 200s, 400s were used. The results are shown in the table 8.

Table 8: Results of the observation of the second test under the optical microscope.

Exposure time (s)	Structures observed in the optical microscope
100	
200	
400	

The results of this test are in accordance with the previous results obtained with test 1.

It is possible to see that with the increase of the exposure time the SU-8 surface becomes smoother. However, it is also observed that for a longer exposure time (400 s) the definition of the smaller structures is not ideal because the SU-8 suffers a melting in that zone.

#### 4.2.2 Soft lithography

Figure 26 shows the result of using the soft lithography technique. The PDMS mold contains the geometry that was in the SU-8 master used.

To obtain this result the SU-8 master was produced and placed in a petri dish. The PDMS was then leached with curing agent in the petri dish with the master and taken to the oven for 20 minutes at 80°C. The mold in PDMS was removed from the oven, cut into the desired shape, the holes were made

for the inlets and outlets and the channels were closed using a glass and the Barrel etcher machine to definitively bond them with the plasma treatment technique.

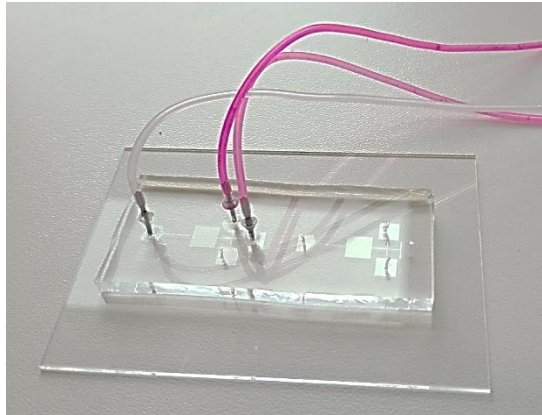


Figure 26: Image of a microdevice made by Soft Lithography.

### 4.3 Conclusions

The results obtained from this study have shown that by using the photolithography equipment located at the *Microproduction and Technical Optics Laboratory*, at Jade University of Applied Sciences, the most appropriate exposure time to produce SU-8 master molds is 200s. After establishing the photolithography protocol with this exposure time all SU-8 structures were very similar and quite satisfactory. In addition, it was observed that all the walls of SU-8 master molds are vertical. It was noticed that masters who needed more cleaning time (developer and isopropanol) were more likely to be damaged when the PDMS mold was made.

Regarding the microfluidic devices produced by using the soft lithography procedure and the devices were extremely satisfactory and it was possible to perform blood flow visualizations and measure the deformation of cells in complex geometries such as bifurcations.

## 5. STUDY OF BLOOD FLOW IN MICROCHANNELS WITH DIVERGING BIFURCATIONS

Blood is a fluid composed primarily of red blood cells (RBCs) suspended in the plasma. RBCs have a complex structure that gives blood unique characteristics at the microscale level. Blood studies in microchannels have been conducted over the years for a more comprehensive characterization of the blood flow properties at a microscale level [39].

In this work the blood was studied in microchannels with diverging bifurcations. Three different geometries (figure 27) were used in order to understand the influence of the bifurcation angle on the flow and deformability of RBCs.

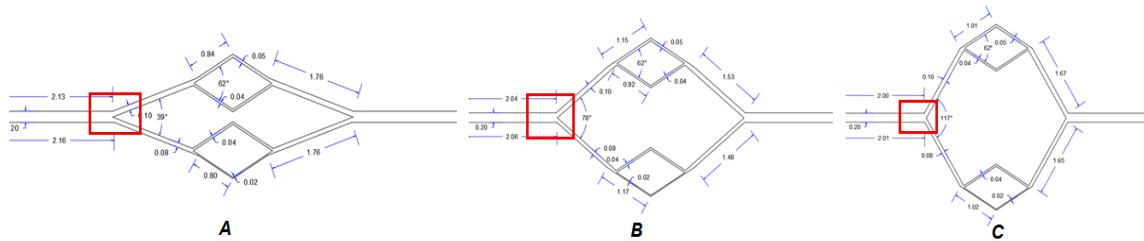


Figure 27: Geometries used in this the study with different angles: 39° (A), 78° (B), 117° (C).

### 5.1 Materials and Methods

For the microfluidic experiments the setup consisted of an inverted microscope (IX71, Olympus) and a high-speed camera (FASTCAM SA3, Photron). The device was placed in the stage of the microscope and a syringe pump was used to produce a constant flow rate of 5  $\mu\text{l}/\text{min}$  (figure 28). The hematocrit used for the study was 1% (a sample was prepared with 1ml of RBCs and 99 ml of Dextran).



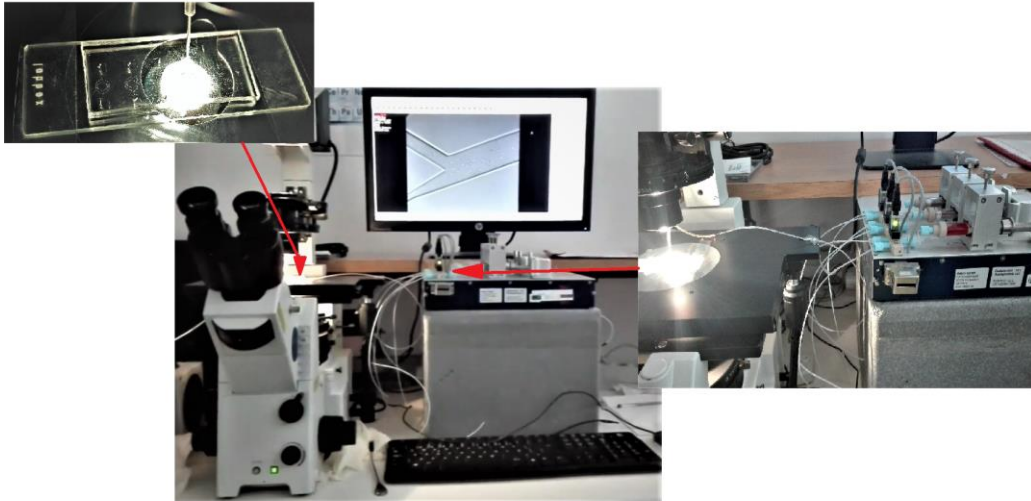


Figure 28: Experimental set up used in the microfluidic experiments.

The parameters used in the study are shown in table 9.

Table 9: Parameters used in the study.

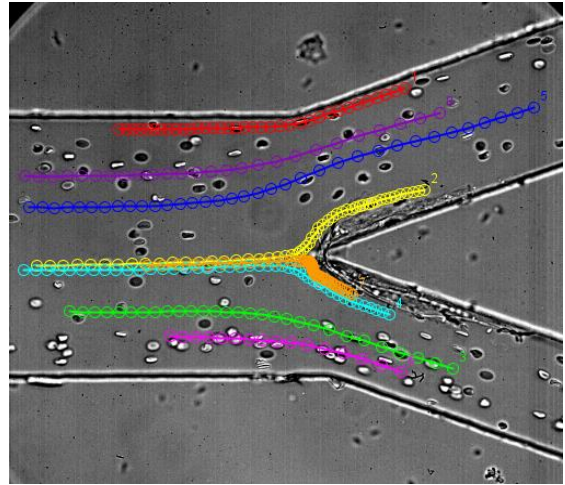
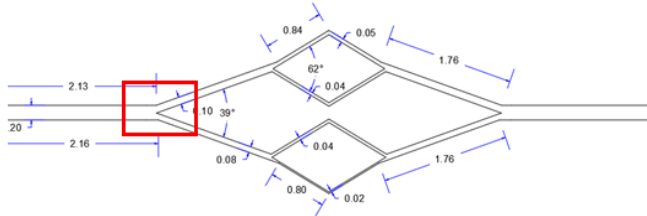
Parameters	Values
Frames	2000 fps
Resolution	1024x1024
Hematocrit (Hct)	1%
Flow rate	5 $\mu$ l/min

After capturing the motion of the RBC, ImageJ was used to track individual RBCs flowing through the microchannels and to measure the deformation and velocity.

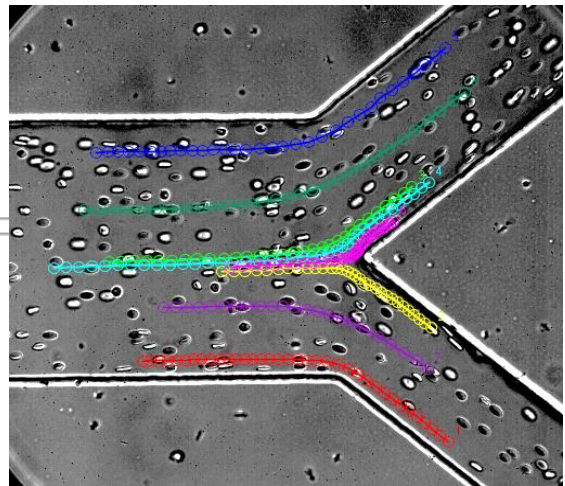
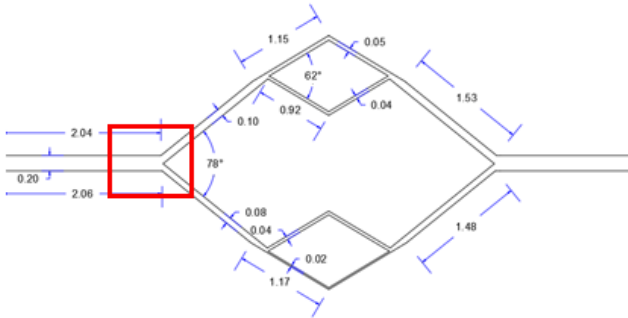
## 5.2 Results and Discussion

In figure 29 it is possible to observe the tracking of cells at the different tested channels with different angles: 39° (A), 78° (B), 117° (C).

A



B



C

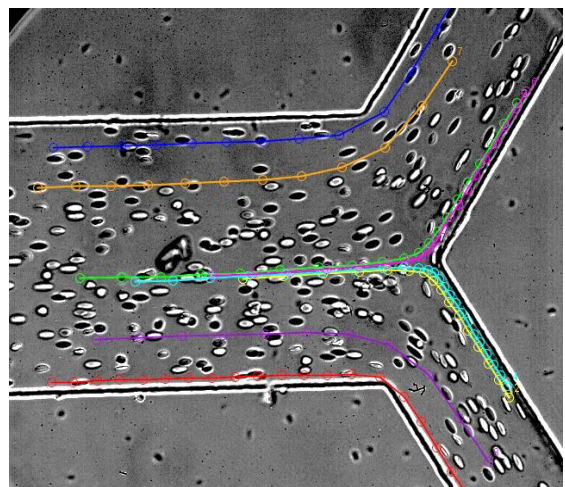
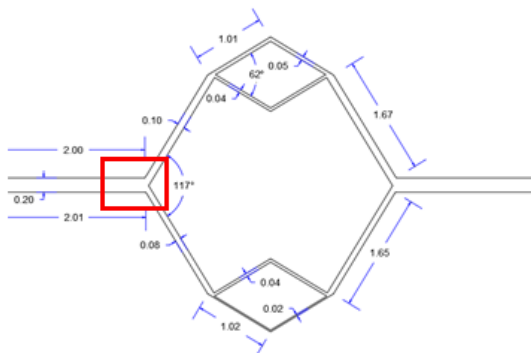
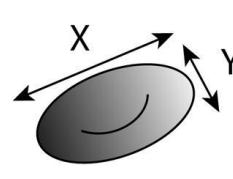


Figure 29: Tracking different cells in the different channels.

To measure the deformation the RBCs it was used the equation of figure 30.



The diagram shows a shaded, biconcave red blood cell. Two double-headed arrows indicate its dimensions: 'X' for the major axis and 'Y' for the minor axis.

$$DI = \frac{X - Y}{X + Y}$$

DI = 0	○
DI = 0.5	◌
DI = 0.8	◌

Figure 30: Equation to measure the deformation of RBCs [40].

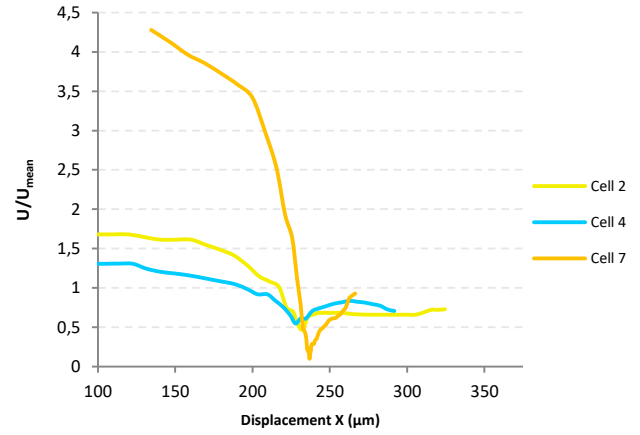
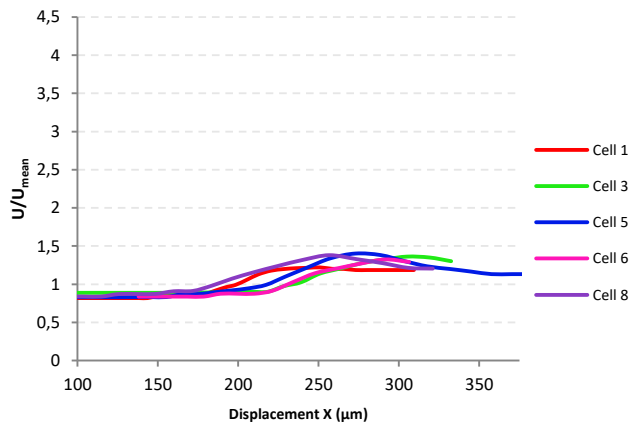
The results of the velocity measurements of different representative RBCs flowing through the tested microchannels can be found in figure 31.

“Far from the apex”

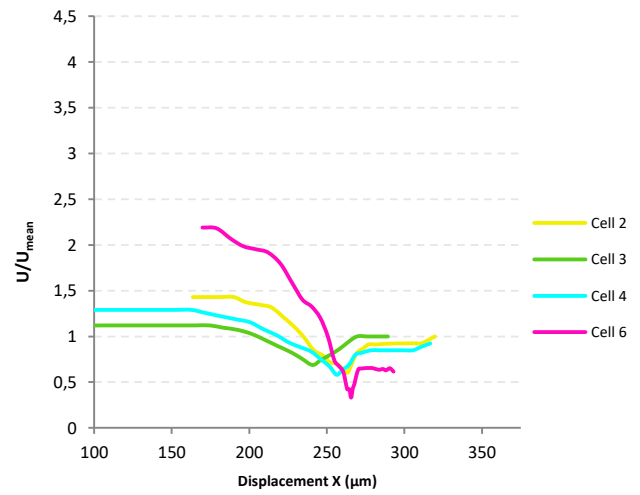
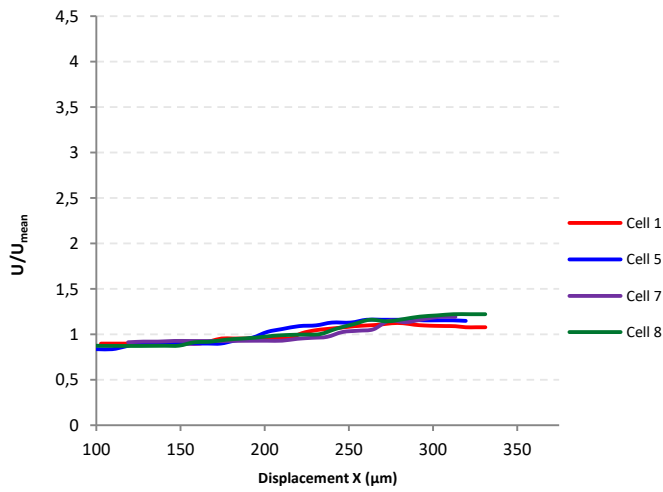
Velocity of the RBCs

“Around the apex”

A



B



C

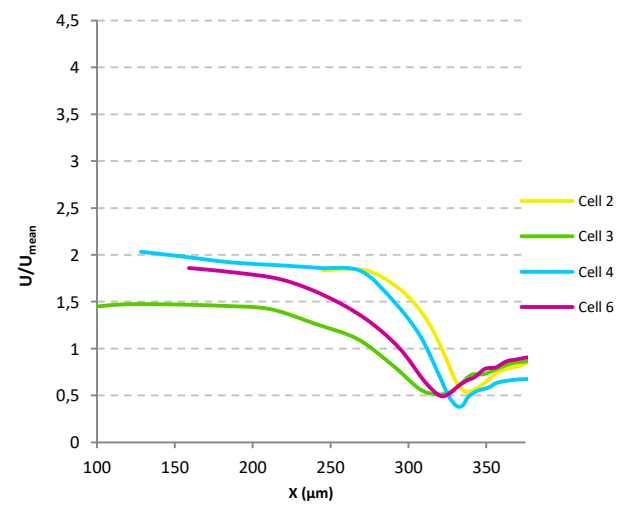
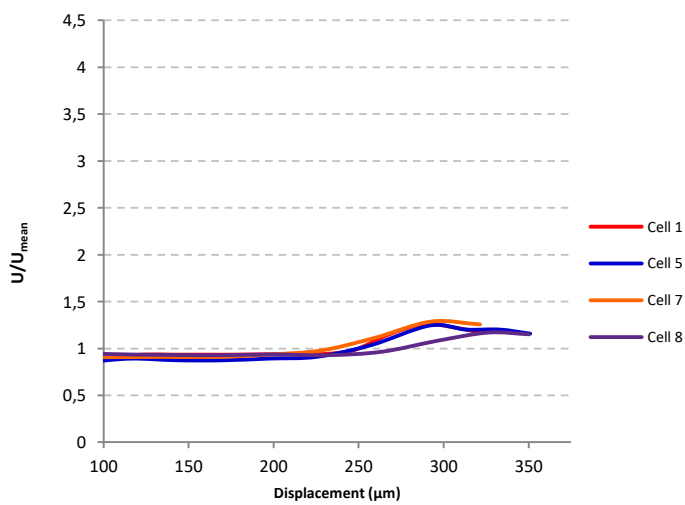


Figure 31: Results of the velocity measurements of different representative RBCs.

Overall, the RBCs that are not in the center of the channel (left figure) suffer an increase in velocity after the bifurcation due to the decrease size of the daughter branches. The RBCs that are flowing in the center of the parent channel (right figure) suffer an abrupt decrease of the velocity around the apex zone and then increase again when the cells enter the daughter branches. This abrupt reduction of the velocities at the apex is mainly due to the presence of a stagnant flow region.

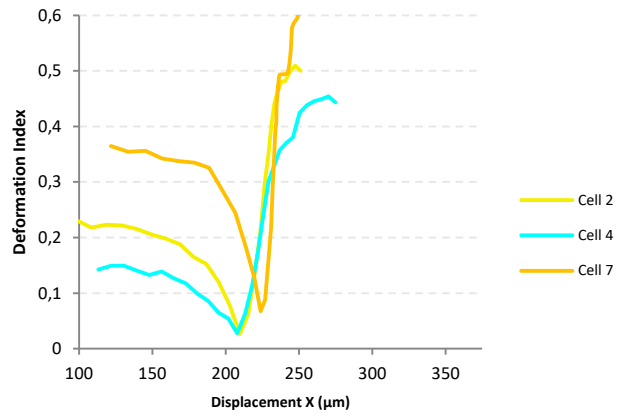
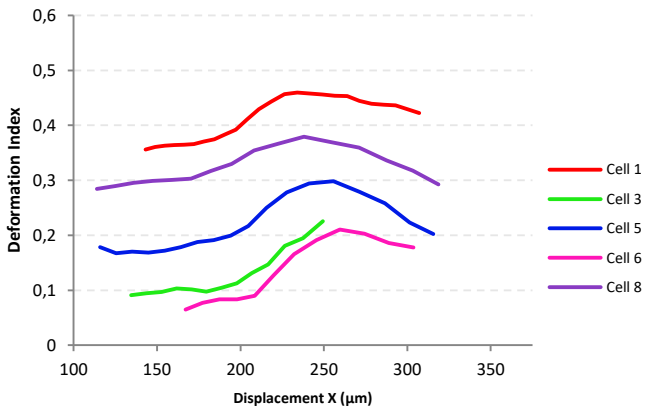
In figure 32, it is shown the deformability measurements of different representative RBCs flowing through the tested microchannels.

"Far from the apex"

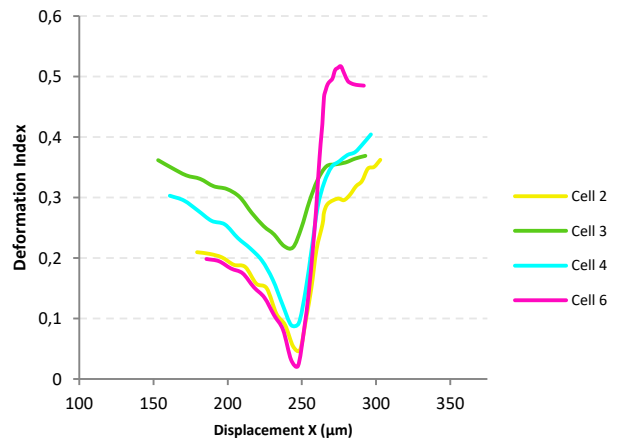
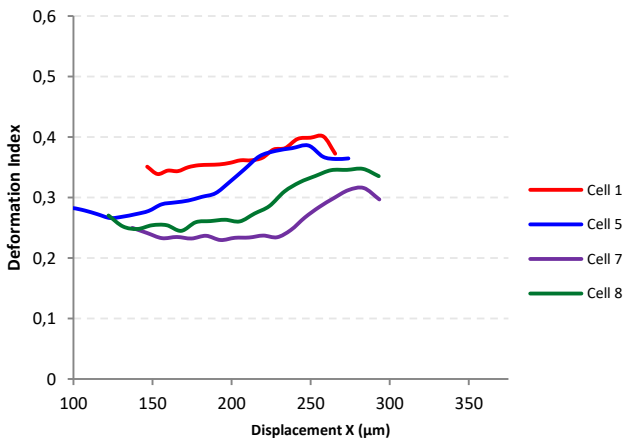
Deformability of RBCs

"Around the apex"

A



B



C

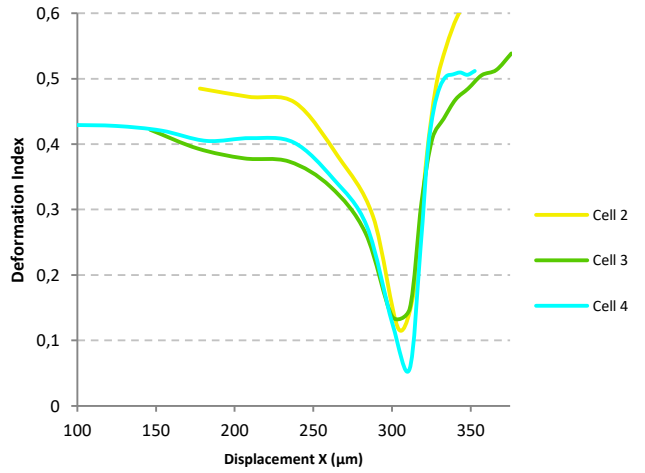
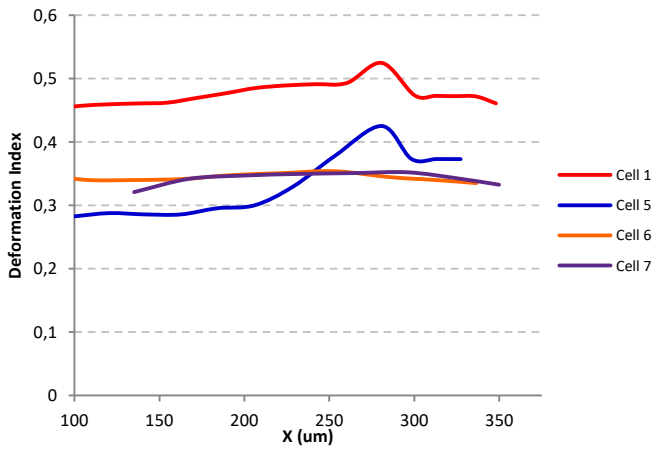


Figure 32: Results of the deformability measurements of different representative RBCs.

Overall, the results from figure 32 shows that the cells that are not in the center of the channel (left) tend to suffer a slight increase of the deformation index (DI) followed by a small decrease. In contrast, the RBCs located at the center of the parent channel suffer an abrupt decrease followed by an exponential increase of the DI around the apex zone.

In figure 33 it is possible to compare the deformation of RBCs flowing at channels with divergent bifurcations and with different angles.

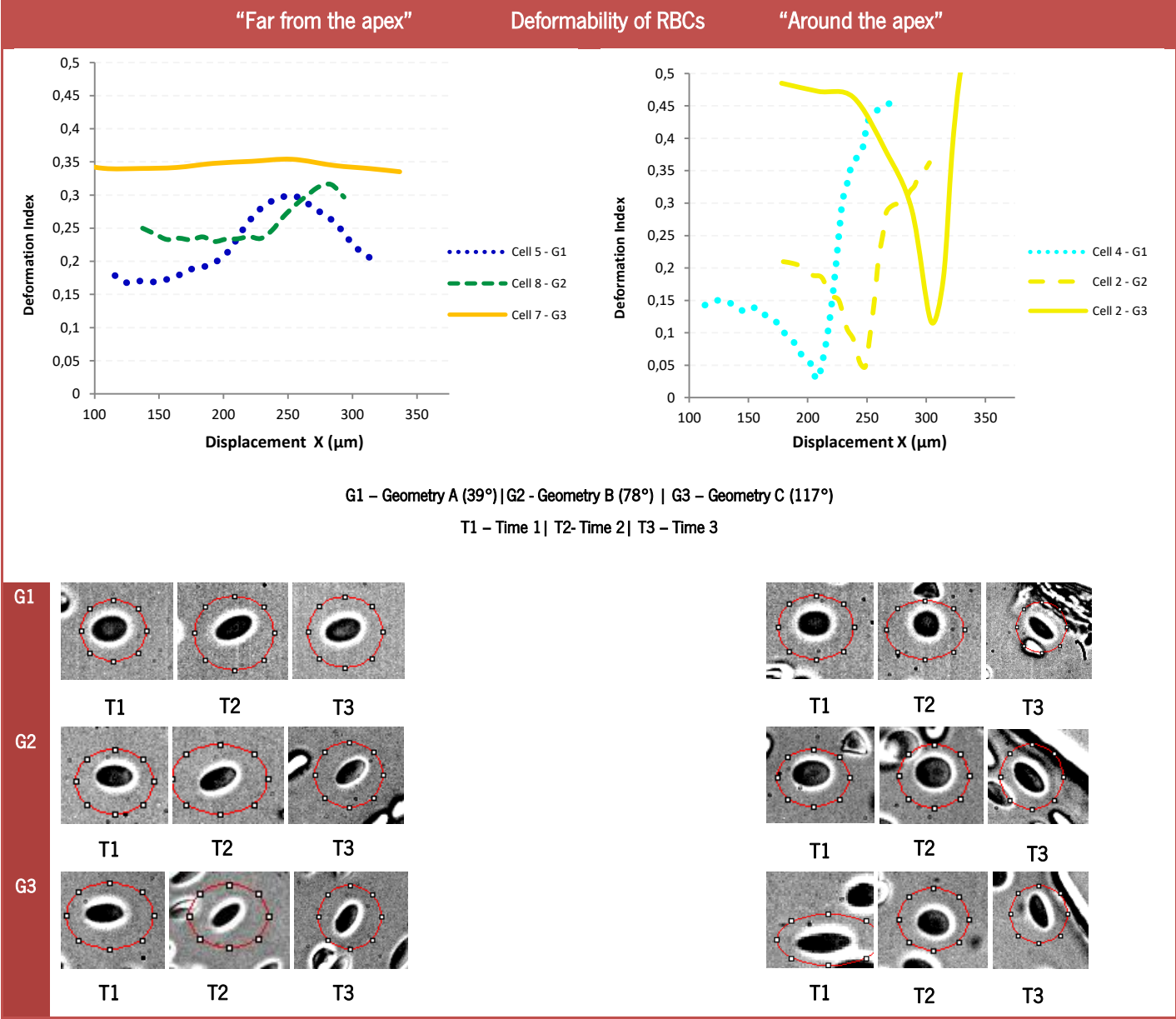


Figure 33: Deformation of cells flowing at channels with divergent bifurcations and with different angles.

Overall, the results from figure 33 indicate that the cells (cell 7, G3) flowing far from the apex and at the geometry C (117°) do not suffer big deformability. In contrast, the RBCs flowing around the apex that suffer the highest abrupt decrease of the deformability are the cells (cell 2, G3) flowing at the geometry C (117°).

### 5.3 Conclusions

Overall, the RBCs that are not flowing at the center of the parent channel tend to suffer an increase in their velocity downstream the bifurcation due to the decrease size of the daughter branches. In addition, these RBCs tend to suffer a slight increase of their deformability followed by a small decrease. Regarding the RBCs that are flowing around the center of the parent channel, they tend to suffer an abrupt decrease of the velocity around the apex zone and then they tend to increase again when the RBCs enter the daughter branches. Additionally, these RBCs suffer an abrupt decrease followed by an exponential increase of the DI around the apex zone.

The results obtained from this study clearly indicate that stagnation region located at the bifurcation apex strongly influence both RBCs velocity and deformability. Apparently from the flow visualizations, this stagnant zone also seems to influence the orientation of the RBCs as the cells flowing around this region seems to not only to deform but also to rotate. Further work needs to be performed in order to clarify this latter phenomenon.

The results also indicate that for the case of the RBCs flowing around the apex the ones that suffer the highest abrupt decrease of the deformability are the RBCs flowing at the geometry with biggest angle (117°).



## 6. CONCLUSIONS AND FUTURE WORK

### 6.1 Conclusions

The main objectives of this master thesis are the development of a blood analogue fluid and the development and manufacture of microchannels with bifurcations to study the flow behavior of individual RBCs.

In the first part of this work, flexible microparticles were produced to mimic the red blood cells. It was possible to produce particles similar in size to RBCs and deformable. The production process has been optimized allowing rapid manufacturing. It was found that by increasing the frequency of the device (Encapsulator B-395 Pro) generates more microspheres of the desired size. The best concentrations for the hardening solution are 0.2M Calcium Chloride and 0.2% TWEEN 80.

After the development of the blood analogue fluid, by using the photolithography and soft lithography techniques microchannels were successfully manufactured. The technique with the most critical procedure was the photolithography and it is important to obtain good results because the master mold has a lot of influence on the quality of the microchannels. Thus, several tests were done to find the best protocol. It has been found that the exposure time has a great influence on the master molds and that the best time is about 200s.

The manufactured microchannels were used to study the flow behavior of individual RBCs. These devices contain diverging bifurcations with different amplitudes: geometry A has a diverging bifurcation with an angle of  $39^\circ$ , the geometry B has an angle of  $78^\circ$  and the geometry C has an angle of  $117^\circ$ . The flow visualization study was mainly focused on the trajectories of the RBCs and it was observed that their trajectories are identical at the different channels. Overall, the results clearly indicate that stagnation region located at the bifurcation apex strongly influence both RBCs velocity and deformability. Apparently from the flow visualizations, this stagnant zone also seems to influence the orientation of the RBCs as the cells flowing around this region are submitted to a complex flow phenomenon where they seem to undergo both deformation and rotational motions.

In addition, the results indicate that for the case of the RBCs flowing around the apex the ones that suffer the highest abrupt decrease of the DI are the RBCs flowing at the geometry with biggest angle ( $117^\circ$ ). Further work needs to be performed in order to clarify these flow phenomena.

In general, the results presented here provide an important contribution to the field of blood analogues, microfluidics and microcirculation.

## 6.2 Future work

As future work on the blood analogue fluid development, it is important to find a good filtration system to obtain at the end microparticles with dimensions similar to the red blood cells. After obtaining a filtered sample it is necessary to study the flow of this blood analogue in microchannels and compare it with the in vitro blood flows.

It would also be interesting to continue to study the flow behavior of individual RBCs since there are phenomena that are not yet fully understood. Apparently in the bifurcations the cells in addition to the deformation also suffer rotation. To better understand the effect, more tests would be needed.

Another interesting work is to study the flow of rigid microparticles or rigid RBCs (mimicking pathological cells) and compare them with the results obtained from this present study.

## BIBLIOGRAFIA

- [1] InnerBody. (2018). *Cardiovascular System - Human Veins, Arteries, Heart*. [online] Available at: <http://www.innerbody.com/image/cardov.html#continued> [Accessed 9 May 2018].
- [2] Biology Discussion. (2018). Blood: Functions, Properties and Groups. [online] Available at: <http://www.biologydiscussion.com/blood/blood-functions-properties-and-groups/44044> [Accessed 9 May 2018].
- [3] myVMC. (2018). Composition of blood (blood cells, electrolytes, proteins) | myVMC. [online] Available at: <https://www.myvmc.com/anatomy/blood-function-and-composition/> [Accessed 9 May 2018].
- [4] Onlinebiologynotes.com. (2018). Blood: composition, properties and functions -. [online] Available at: <http://www.onlinebiologynotes.com/blood-composition-properties-functions/> [Accessed 9 May 2018].
- [5] Encyclopedia.lubopitko-bg.com. (2018). Blood. Functions of the Blood. Structure of the Blood. [online] Available at: [http://encyclopedia.lubopitko-bg.com/The\\_Blood.html](http://encyclopedia.lubopitko-bg.com/The_Blood.html) [Accessed 9 May 2018].
- [6] Turkupetcentre.net. (2018). TPC - Hematocrit. [online] Available at: <http://www.turkupetcentre.net/petanalysis/hematocrit.html> [Accessed 9 May 2018].
- [7] Austincc.edu. (2018). Associate Degree Nursing Physiology Review. [online] Available at: <http://www.austincc.edu/apreview/PhysText/Blood.htm> [Accessed 9 May 2018].
- [8] Baskurt, O. and Meiselman, H. (2003). Blood Rheology and Hemodynamics. *Seminars in Thrombosis and Hemostasis*, 29(5), pp.435-450.
- [9] Encyclopedia Britannica. (2018). Fluid | physics. [online] Available at: <https://www.britannica.com/science/fluid-physics#ref176741> [Accessed 17 May 2018].
- [10] Lima R. "Apontamentos de Termodinâmica e Mecânica dos Fluidos", Mestrado Integrado de Engenharia e Gestão Industrial, UMinho, Guimarães, 2018.
- [11] R. Lima, T. Ishikawa, Y. Imai and T. Yamaguchi "BLOOD FLOW BEHAVIOR IN MICROCHANNELS: PAST, CURRENT AND FUTURE TRENDS. Single and two-Phase Flows on Chemical and Biomedical Engineering, Dias et al.(Eds), Bentham Science, 513-547, 2012
- [12] R. Lima, T. Ishikawa, Y. Imai and T. Yamaguchi. "BLOOD FLOW BEHAVIOR IN MICROCHANNELS: PAST, CURRENT AND FUTURE TRENDS. Single and two-Phase Flows on Chemical and Biomedical Engineering, Dias et al.(Eds), Bentham Science, 513-547, 2012
- [13] Shen, Z., Coupier, G., Kaoui, B., Polack, B., Harting, J., Misbah, C. and Podgorski, T. (2016). Inversion of hematocrit partition at microfluidic bifurcations. *Microvascular Research*, 105, pp.40-46.
- [14] Tripathi, S., Varun Kumar, Y., Prabhakar, A., Joshi, S. and Agrawal, A. (2015). Passive blood plasma separation at the microscale: a review of design principles and microdevices. *Journal of Micromechanics and Microengineering*, 25(8), p.083001.
- [15] P.C. Sousa, I.S. Pinho, F.T. Pinho, M.S.N. Oliveira, and M.A. Alves, *Flow of a blood analogue solution through microfabricated hyperbolic contractions*. In: *Computational Vision and Medical Image Processing. Computational Methods in Applied Sciences*, 19, Springer, pp 265-279, 2011.
- [16] L. Campo-Deaño, R. P. A. Dullens, D. G. A. L. Aarts, F. T. Pinho, and M. S. N. Oliveira, Viscoelasticity of blood and viscoelastic blood analogues for use in polydimethylsiloxane in vitro models of the circulatory system. *Biomicrofluidics* 7(3), 034102, 2013.
- [17] Diana Pinho, Laura Campo-Deaño, Rui Lima, and Fernando T. Pinho, In vitro particulate analogue fluids for experimental studies of rheological and hemorheological behavior of glucose-rich RBC suspensions. *Biomicrofluidics* 11, 054105 2017;
- [18] BN Muñoz-Sánchez, SF Silva, D Pinho, EJ Veja, R Lima, Generation of micro-sized PDMS particles by a flow focusing technique for biomicrofluidics applications. *Biomicrofluidics*, 10, 014122 (2016);

- [19] Calejo, J.; Pinho, D.; Galindo-Rosales, F.J.; Lima, R.; Campo-Deaño, L. Particulate Blood Analogues Reproducing the Erythrocytes Cell-Free Layer in a Microfluidic Device Containing a Hyperbolic Contraction. *Micromachines* 2016, 7, 4, 2016.
- [20] Faustino V., Catarino S. O., Lima R. and Minas G., Biomedical microfluidic devices by using low-cost fabrication techniques: A review, *Journal of Biomechanics* 49 (11), 2280–2292, 2016
- [21] Rodrigues R. O., Lima R., Gomes H. T., Silva A. M. T., Polymer microfluidic devices: an overview of fabrication methods, *U. Porto Journal of Engineering* 1 (1), 67-79, 2015.
- [22] Geschke, O., Klank, H. and Tellemann, P. (2010). *Microsystem Engineering of Lab-on-a-chip Devices*. Vch Verlagsgesellschaft Mbh.
- [23] Elveflow. (2018). Fabrication of glass and film photomasks - Elveflow. [online] Available at: <https://www.elveflow.com/microfluidic-tutorials/soft-lithography-reviews-and-tutorials/microfluidic-device-fabrication/fabrication-of-glass-and-film-photomasks/> [Accessed 23 May 2018].
- [24] Microchemicals.com. (2018). [online] Available at: [https://www.microchemicals.com/technical\\_information/exposure\\_photoresist.pdf](https://www.microchemicals.com/technical_information/exposure_photoresist.pdf) [Accessed 23 May 2018].
- [25] Halbleiter.org. (2018). Exposure and resist coating - Photolithography - Semiconductor Technology from A to Z - Halbleiter.org. [online] Available at: <https://www.halbleiter.org/en/photolithography/exposure/> [Accessed 23 May 2018].
- [26] Microchemicals.com. (2018). Photoresists AZ and MicroChemicals TI resists. [online] Available at: <https://www.microchemicals.com/products/photoresists.html> [Accessed 23 May 2018].
- [27] Wormbook.org. (2018). Microfluidics as a tool for *C. elegans* research. [online] Available at: [http://www.wormbook.org/chapters/www\\_microfluidics/microfluidics.html](http://www.wormbook.org/chapters/www_microfluidics/microfluidics.html) [Accessed 23 May 2018].
- [28] P. C. Sousa, F. T. Pinho, M. S. N. Oliveira, and M. A. Alves, “Extensional flow of blood analog solutions in microfluidic devices,” *Biomicrofluidics*, vol. 5, no. 1, pp. 1–19, 2011.
- [29] Buchi.com. (2018). Nano Spray Dryer B-90 HP | buchi.com. [online] Available at: <https://www.buchi.com/en/products/spray-drying-and-encapsulation/nano-spray-dryer-b-90-hp> [Accessed 23 Nov. 2018].
- [30] Buchi.com. (2018). *Encapsulator B-395 Pro* | buchi.com. [online] Available at: <https://www.buchi.com/en/products/spray-drying-and-encapsulation/encapsulator-b-395-pro> [Accessed 23 Nov. 2018].
- [31] manualsdir.com. (2018). BUCHI Nano Spray Dryer B-90 - Manual (Page 26). [online] Available at: <http://www.manualsdir.com/manuals/656065/buchi-nano-spray-dryer-b-90.html?page=26> [Accessed 23 Nov. 2018].
- [32] Johnmorrisgroup.com. (2018). [online] Available at: [https://www.johnmorrisgroup.com/Content/Attachments/150414/B-395\\_OM\\_en\\_C.pdf](https://www.johnmorrisgroup.com/Content/Attachments/150414/B-395_OM_en_C.pdf) [Accessed 23 Nov. 2018].
- [33] Lee, K. and Mooney, D. (2012). Alginate: Properties and biomedical applications. *Progress in Polymer Science*, 37(1), pp.106-126.
- [34] Campos, S. (2017). *Measurement of red blood cells flowing through microchannels with complex geometries*. Master. University of Minho.
- [35] completo, V. (2018). Lâmpadas fluorescentes e os efeitos tóxicos. [online] Quipibid.blogspot.com. Available at: <http://quipibid.blogspot.com/2014/07/lampadas-fluorescentes-e-os-efeitos.html> [Accessed 27 Nov. 2018].
- [36] Elveflow. (2018). *SU-8 photolithography: Baking* - Elveflow. [online] Available at: <https://www.elveflow.com/microfluidic-tutorials/soft-lithography-reviews-and-tutorials/how-to-get-the-best-process/su-8-photolithography-baking/> [Accessed 5 Jul. 2018].
- [37] Bme240.eng.uci.edu. (2018). *Device Fabrication and Design*. [online] Available at: <http://bme240.eng.uci.edu/students/08s/jtluo/Device%20Fabrication.htm> [Accessed 27 Nov. 2018].

- [38] Henniker Plasma Treatment. (2018). Plasma treatment of PDMS for microfluidic applications. [online] Available at: <https://plasmatreatment.co.uk/henniker-plasma-technology/plasma-treatments/plasma-surface-activation-to-improve-adhesion/plasma-treatment-of-pdms/> [Accessed 27 Nov. 2018].
- [39] Leble, V., Lima, R., Dias, R., Fernandes, C., Ishikawa, T., Imai, Y. and Yamaguchi, T. (2011). Asymmetry of red blood cell motions in a microchannel with a diverging and converging bifurcation. *Biomicrofluidics*, 5(4), p.044120.
- [40] Bento, D., Rodrigues, R., Faustino, V., Pinho, D., Fernandes, C., Pereira, A., Garcia, V., Miranda, J., and Lima, R. (2018). Deformation of Red Blood Cells, Air Bubbles, and Droplets in Microfluidic Devices: Flow Visualizations and Measurements. *Micromachines* 9, 151.



# ANNEX I – SU-8 DATASHEET



www.microchem.com

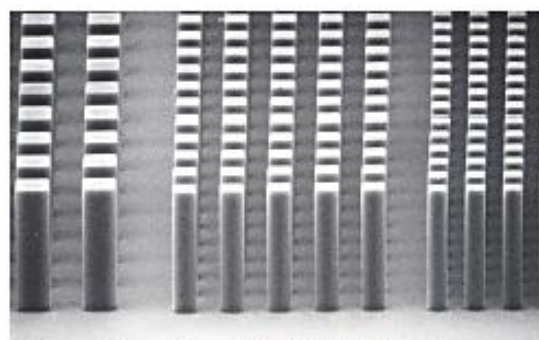
## SU-8 2000

### Permanent Epoxy Negative Photoresist

#### PROCESSING GUIDELINES FOR:

#### SU-8 2025, SU-8 2035, SU-8 2050 and SU-8 2075

SU-8 2000 is a high contrast, epoxy based photoresist designed for micromachining and other microelectronic applications, where a thick, chemically and thermally stable image is desired. SU-8 2000 is an improved formulation of SU-8, which has been widely used by MEMS producers for many years. The use of a faster drying, more polar solvent system results in improved coating quality and increases process throughput. SU-8 2000 is available in twelve standard viscosities. Film thicknesses of 0.5 to >200 microns can be achieved with a single coat process. The exposed and subsequently thermally cross-linked portions of the film are rendered insoluble to liquid developers. SU-8 2000 has excellent imaging characteristics and is capable of producing very high aspect ratio structures. SU-8 2000 has very high optical transmission above 360 nm, which makes it ideally suited for imaging near vertical sidewalls in very thick films. SU-8 2000 is best suited for permanent applications where it is imaged, cured and left on the device.



10 um features, 50 um SU-8 2000 coating

#### SU-8 2000 Features

- High aspect ratio imaging
- 0.5 to > 200 µm film thickness in a single coat
- Improved coating properties
- Faster drying for increased throughput
- Near UV (350-400 nm) processing
- Vertical sidewalls

#### Processing Guidelines

SU-8 2000 photoresist is most commonly exposed with conventional UV (350-400 nm) radiation, although i-line (365 nm) is the recommended wavelength. SU-8 2000 may also be exposed with e-beam or x-ray radiation. Upon exposure, cross-linking proceeds in two steps (1) formation of a strong acid during the exposure step, followed by (2) acid-catalyzed, thermally driven epoxy cross-linking during the post exposure bake (PEB) step. A normal process is: spin coat, soft bake, expose, PEB, followed by develop. A controlled hard bake is recommended to further cross-link the imaged SU-8 2000 structures when they will remain as part of the device. The entire process should be optimized for the specific application. The baseline information presented here is meant to be used as a starting point for determining a process.

#### Process Flow



Table 1. SU-8 2000 Viscosity

SU-8 2000	% Solids	Viscosity (cSt)	Density (g/ml)
2025	68.55	4500	1.219
2035	69.95	7000	1.227
2050	71.65	12900	1.233
2075	73.45	22000	1.236

**Substrate Preparation**

To obtain maximum process reliability, substrates should be clean and dry prior to applying SU-8 2000 resist. For best results, substrates should be cleaned with a piranha wet etch (using H<sub>2</sub>SO<sub>4</sub> & H<sub>2</sub>O<sub>2</sub>) followed by a de-ionized water rinse. Substrates may also be cleaned using reactive ion etching (RIE) or any barrel asher supplied with oxygen. Adhesion promoters are typically not required. For applications that include electroplating, a pre-treatment of the substrate with MCC Primer 80/20 (HMDS) is recommended.

**Coat**

SU-8 2000 resists are available in twelve standard viscosities. This processing guideline document addresses four products: SU-8 2025, SU-8 2035, SU-8 2050 and SU-8 2075. Figure 1. provides the information required to select the appropriate SU-8 2000 resist and spin conditions to achieve the desired film thickness.

**Recommended Program**

- 1.) Dispense 1ml of resist for each inch (25mm) of substrate diameter.
- 2.) Spin at 500 rpm for 5-10 seconds with acceleration of 100 rpm/second.
- 3.) Spin at 2000 rpm for 30 seconds with acceleration of 300 rpm/second.

**Edge Bead Removal (EBR)**

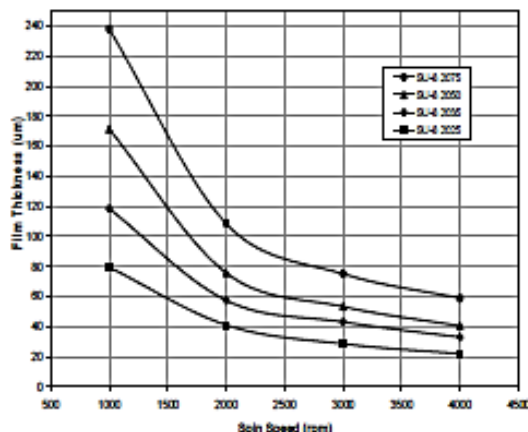
During the spin coat process step, a build up of photoresist may occur on the edge of the substrate. In order to minimize contamination of the hotplate, this thick bead should be removed. This can be accomplished by using a small stream of solvent (MicroChem's EBR PG) at the edge of the wafer either at the top or from the bottom. Most automated spin coaters now have this feature and can be programmed to do this automatically.

By removing any edge bead, the photomask can be placed into close contact with the wafer, resulting in improved resolution and aspect ratio.

**Soft Bake**

A level hotplate with good thermal control and uniformity is recommended for use during the Soft Bake step of the process. Convection ovens are not recommended. During convection oven baking, a skin may form on the resist. This skin can inhibit the evolution of solvent, resulting in incomplete drying of the film and/or extended bake times. Table 2. shows the recommended Soft Bake temperatures and times for the various SU-8 2000 products at selected film thicknesses.

Figure 1. SU-8 2000 Spin Speed versus Thickness



*Note: To optimize the baking times/conditions, remove the wafer from the hotplate after the prescribed time and allow it to cool to room temperature. Then, return the wafer to the hotplate. If the film 'wrinkles', leave the wafer on the hotplate for a few more minutes. Repeat the cool-down and heat-up cycle until 'wrinkles' are no longer seen in the film.*

THICKNESS microns	SOFT BAKE TIMES	
	(65°C) minutes	(95°C) minutes
25 - 40	0 - 3	5 - 6
45 - 80	0 - 3	6 - 9
85 - 110	5	10 - 20
115 - 150	5	20 - 30
160 - 225	7	30 - 45

Table 2. Soft Bake Times



### Optical Parameters

The dispersion curve and Cauchy coefficients are shown in Figure 3. This information is useful for film thickness measurements based on ellipsometry and other optical measurements.

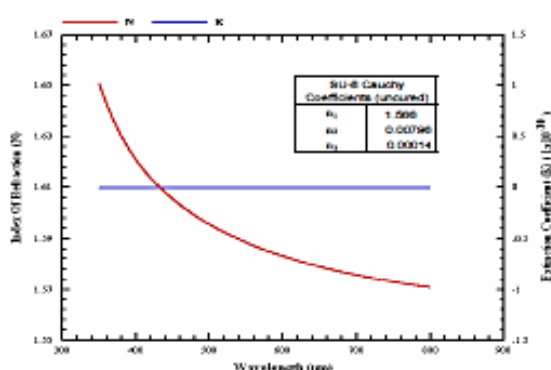


Figure 3. Cauchy Coefficients

### Exposure

To obtain vertical sidewalls in the SU-8 2000 resist, we recommend the use of a long pass filter to eliminate UV radiation below 350 nm. With the recommended filter (PL-380-LP) from Omega Optical ([www.omegafilters.com](http://www.omegafilters.com)) or Asahi Technoglass filters V-42 plus UV-D35 ([www.atgc.co.jp](http://www.atgc.co.jp)), an increase in exposure time of approximately 40% is required to reach the optimum exposure dose.

*Note: With optimal exposure, a visible latent image will be seen in the film within 5-15 seconds after being placed on the PEB hotplate and not before. An exposure matrix experiment should be performed to determine the optimum dosage.*

THICKNESS microns	EXPOSURE ENERGY mJ/cm <sup>2</sup>
25 - 40	150 - 160
45 - 80	150 - 215
85 - 110	215 - 240
115 - 150	240 - 260
160 - 225	260 - 350

Table 3. Exposure Dose

	RELATIVE DOSE
Silicon	1X
Glass	1.5X
Pyrex	1.5X
Indium Tin Oxide	1.5X
Silicon Nitride	1.5 - 2X
Gold	1.5 - 2X
Aluminum	1.5 - 2X
Nickel Iron	1.5 - 2X
Copper	1.5 - 2X
Nickel	1.5 - 2X
Titanium	1.5 - 2X

Table 4. Exposure Doses for Various Substrates

### Post Exposure Bake (PEB)

PEB should take place directly after exposure. Table 5. shows the recommended times and temperatures

*Note: After 1 minute of PEB at 95°C, an image of the mask should be visible in the SU-8 2000 photoresist coating. If no visible latent image is seen during or after PEB this means that there was insufficient exposure, heating or both.*

THICKNESS microns	PEB TIME (65°C)* minutes	PEB TIME (95°C) minutes
25 - 40	1	5 - 6
45 - 80	1 - 2	6 - 7
85 - 110	2 - 5	8 - 10
115 - 150	5	10 - 12
160 - 225	5	12 - 15

\* Optional step for stress reduction

Table 5. Post Exposure Bake Times

### Development

SU-8 2000 photoresist has been designed for use in immersion, spray or spray-puddle processes with MicroChem's SU-8 developer. Other solvent based developers such as ethyl lactate and diacetone alcohol may also be used. Strong agitation is recommended when developing high aspect ratio and/or thick film structures. The recommended development times for immersion processes are given in Table 6. These development times are approximate, since actual dissolution rates can vary widely as a function of agitation

*Note: The use of an ultrasonic or megasonic bath may be helpful when developing out via or hole patterns or structures with tight pitch.*

THICKNESS	DEVELOPMENT TIME
microns	minutes
25 - 40	4 - 5
45 - 75	5 - 7
80 - 110	7 - 10
115 - 150	10 - 15
160 - 225	15 - 17

Table 6. Development Times for SU-8 Developer

**Rinse and Dry**

When using SU-8 developer, spray and wash the developed image with fresh solution for approximately 10 seconds, followed by a second spray/wash with Isopropyl Alcohol (IPA) for another 10 seconds. Air dry with filtered, pressurized air or nitrogen.

*Note: A white film produced during IPA rinse is an indication of underdevelopment of the unexposed photoresist. Simply immerse or spray the substrate with additional SU-8 developer to remove the white film and complete the development process. Repeat the rinse step.*

*The use of an ultrasonic or megasonic bath will energize the solvent and allow for more effective development of the unexposed resist.*

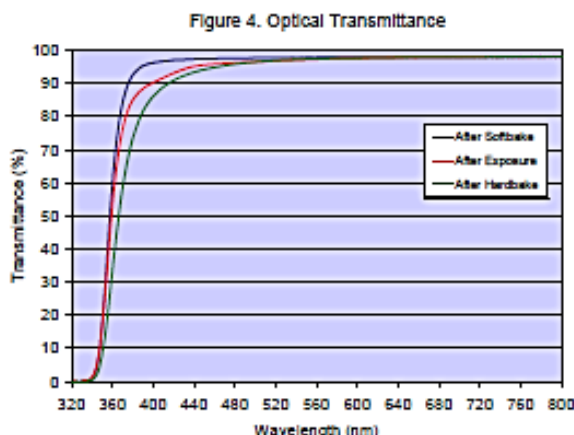
**Physical Properties**

(Approximate values)

Adhesion Strength (mPa) Silicon/Glass/Glass & HMDS	38/35/35
Glass Transition Temperature (T <sub>g</sub> °C), tan δ peak	210
Thermal Stability (°C @ 5% wt. loss)	315
Thermal Conductivity (W/mK)	0.3
Coeff. of Thermal Expansion (CTE ppm)	52
Tensile Strength (Mpa)	60
Elongation at break (εb %)	6.5
Young's Modulus (Gpa)	2.0
Dielectric Constant @ 10MHz	3.2
Water Absorption (% 85°C/85 RH)	0.65

Table 7. Physical Properties

**Optical Properties**



**Process conditions for Figure 4.**

Softbake: 5 minutes at 95°C  
 Exposure: 180 mJ/cm<sup>2</sup>  
 Hardbake: 30 minutes at 300°C

**Hard Bake (cure)**

SU-8 2000 has good mechanical properties. However, for applications where the imaged resist is to be left as part of the final device, a hard bake can be incorporated into the process. This is generally only required if the final device or part is to be subject to thermal processing during regular operation. A hard bake or final cure step is added to ensure that SU-8 2000 properties do not change in actual use. SU-8 2000 is a thermal resin and as such its properties can continue to change when exposed to a higher temperature than previously encountered. We recommend using a final bake temperature 10°C higher than the maximum expected device operating temperature. Depending on the degree of cure required, a bake temperature in the range of 150°C to 250°C and for a time between 5 and 30 minutes is typically used.

*Note: The hard bake step is also useful for annealing any surface cracks that may be evident after development. The recommended step is to bake at 150°C for a couple of minutes. This applies to all film thicknesses.*

### Removal

SU-8 2000 has been designed as a permanent, highly cross-linked epoxy material and it is extremely difficult to remove it with conventional solvent based resist strippers. MicroChem's Remover PG will swell and lift off minimally cross-linked SU-8 2000. However, if OmniCoat (30-100 nm) has been applied, immersion in Remover PG can effect a clean and thorough Lift-Off of the SU-8 2000 material. Fully cured or hard baked SU-8 2000 cannot be removed without the use of OmniCoat.

To remove minimally cross-linked SU-8 2000, or when using OmniCoat: Heat the Remover PG bath to 50-80°C and immerse the substrates for 30-90 minutes. Actual strip time will depend on resist thickness and cross-link density. For more information on MicroChem OmniCoat and Remover PG please see the relevant product data sheets.

To re-work fully cross-linked SU-8 2000: Wafers can be stripped using oxidizing acid solutions such as piranha etch, plasma ash, RIE, laser ablation and pyrolysis.

### Plasma Removal

RIE 200W, 80 sccm O<sub>2</sub>, 8 sccm CF<sub>4</sub>, 100mTorr, 10°C

### Storage

Store SU-8 2000 resists upright and in tightly closed containers in a cool, dry environment away from direct sunlight at a temperature of 40-70°F (4-21°C). Store away from light, acids, heat and sources of ignition. Shelf life is thirteen months from date of manufacture.

### Disposal

SU-8 2000 resists may be included with other waste containing similar organic solvents to be discarded for destruction or reclaim in accordance with local state and federal regulations. It is the responsibility of the customer to ensure the disposal of SU-8 2000 resists and residues made in observance all federal, state, and local environmental regulations.

### Environmental, Health and Safety

Consult the product Material Safety Data Sheet before working with SU-8 2000 resists. Handle with care. Wear chemical goggles, chemical gloves and suitable protective clothing when handling SU-8 2000 resists. Do not get into eyes, or onto skin or clothing. Use with adequate ventilation to avoid breathing vapors or mist. In case of contact with skin, wash affected area with soap and water. In case of contact with eyes, rinse immediately with water and flush for 15 minutes lifting eyelids frequently. Get emergency medical assistance.

The information is based on our experience and is, we believe to be reliable, but may not be complete. We make no guarantee or warranty, expressed or implied, regarding the information, use, handling, storage, or possession of these products, or the application of any process described herein or the results desired, since the conditions of use and handling of these products are beyond our control.

### Disclaimer

Notwithstanding anything to the contrary contained in any sales documentation, e.g., purchase order forms, all sales are made on the following conditions:

All information contained in any MicroChem product literature reflects MicroChem's current knowledge on the subject and is, we believe, reliable. It is offered solely to provide possible suggestions for customer's own experiments and is not a substitute for any testing by customer to determine the suitability of any of MicroChem products for any particular purpose. This information may be subject to revision as new knowledge and experience becomes available, but MicroChem assumes no obligation to update or revise any data previously furnished to a customer; and if currency of data becomes an issue, customer should contact MicroChem requesting updates. Since MicroChem cannot anticipate all variations in actual end uses or in actual end-use conditions, it makes no claims, representations or warranties, express or implied including, without limitation any warranty of merchantability or fitness for a particular purpose; and customer waives all of the same. MicroChem expressly disclaims any responsibility or liability and assumes no responsibility or liability in connection with any use of this information including, without limitation, any use, handling, storage or possession of any MicroChem products, or the application of any process described herein or the results desired or anything relating to the design of the customer's products. Nothing in this publication is to be considered as a license to operate under or a recommendation to infringe any patent right.

### Caution

This product is not designed or manufactured for, nor is it intended for use in any medical device or for any other medical application. Do not use this product in any medical applications [including, without limitation, any permanent implantation in the human body or any animals (other than laboratory animals used for experimental purposes), or contact with internal body fluids or tissues] unless otherwise expressly and specifically provided for in a written contract between MCC and the customer. The complete MicroChem Medical Disclaimer Statement is available upon request or on the MicroChem website at [www.microchem.com](http://www.microchem.com).

# ANNEX II – ALL GEOMETRIES OF MICROCHANNELS PRODUCED AT JADE UNIVERSITY OF APPLIED SCIENCES

